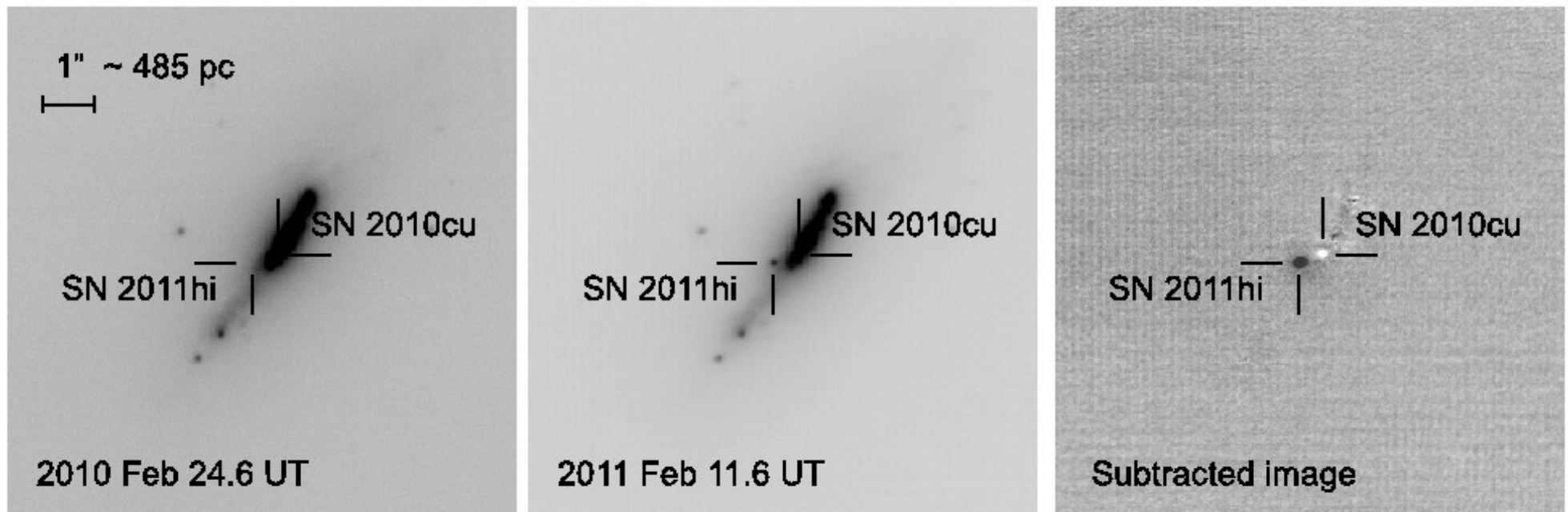


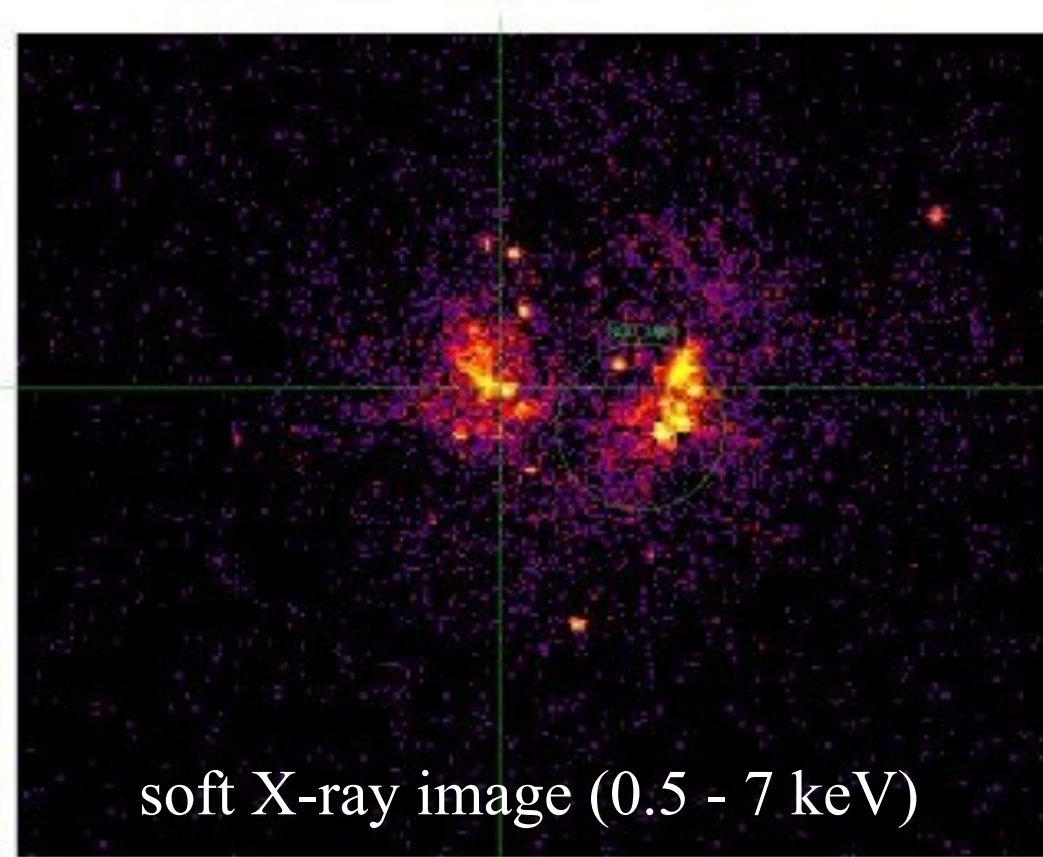
Astronomical imaging & image processing

Seppo Mattila (sepmat@utu.fi)

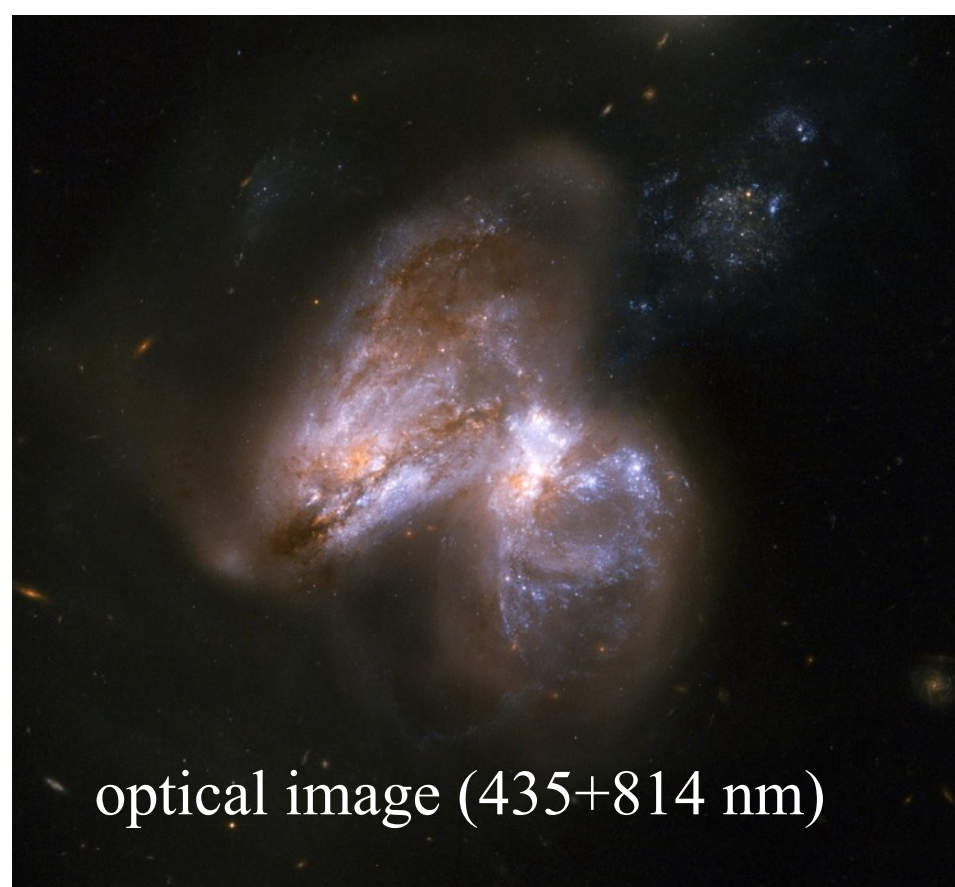
Department of Physics and Astronomy, University of Turku



Examples of astronomical imaging data



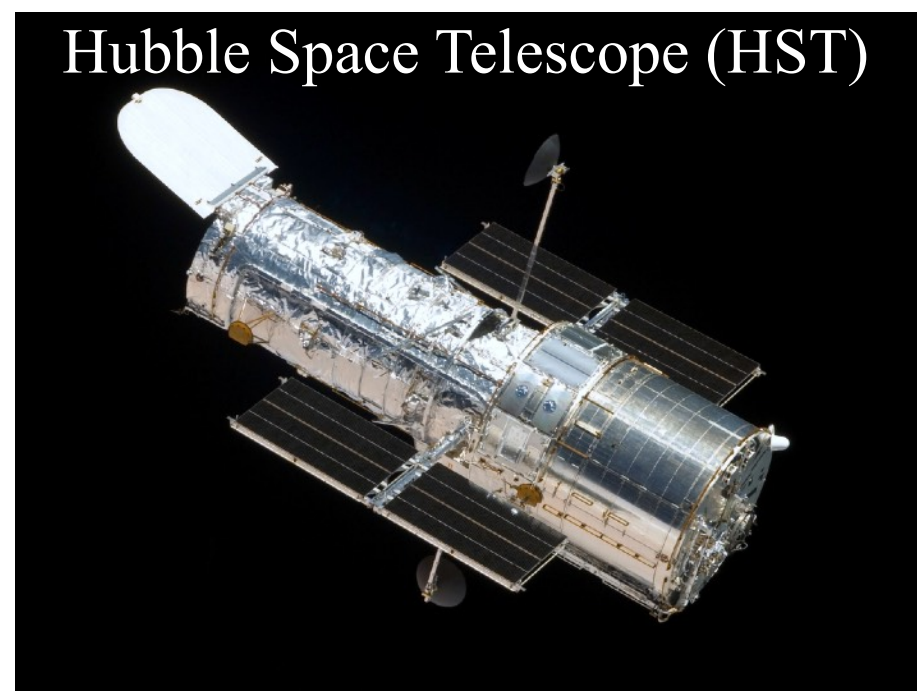
soft X-ray image (0.5 - 7 keV)



optical image (435+814 nm)



NASA Chandra X-ray observatory



Hubble Space Telescope (HST)




Hubble Space Telescope (HST) optical (435 + 814 nm) (PSF FWHM $\sim 0.1''$)

2010O →

2010P ↙

NOT/NOTCam near-infrared (2.2 μm) (PSF FWHM $\sim 1''$)

SN2010O 

SN2010P 

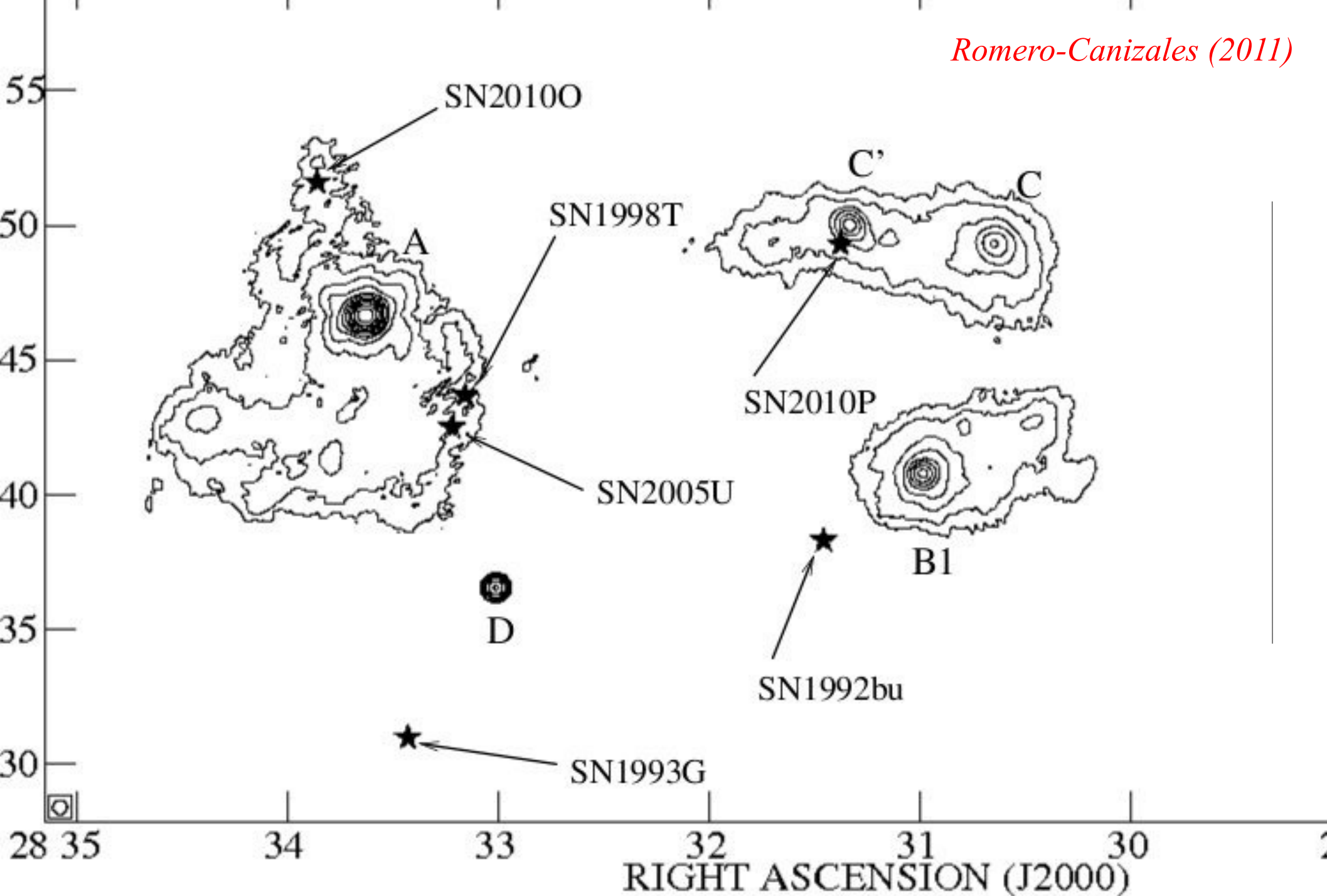
 SN1998T


SN2005U

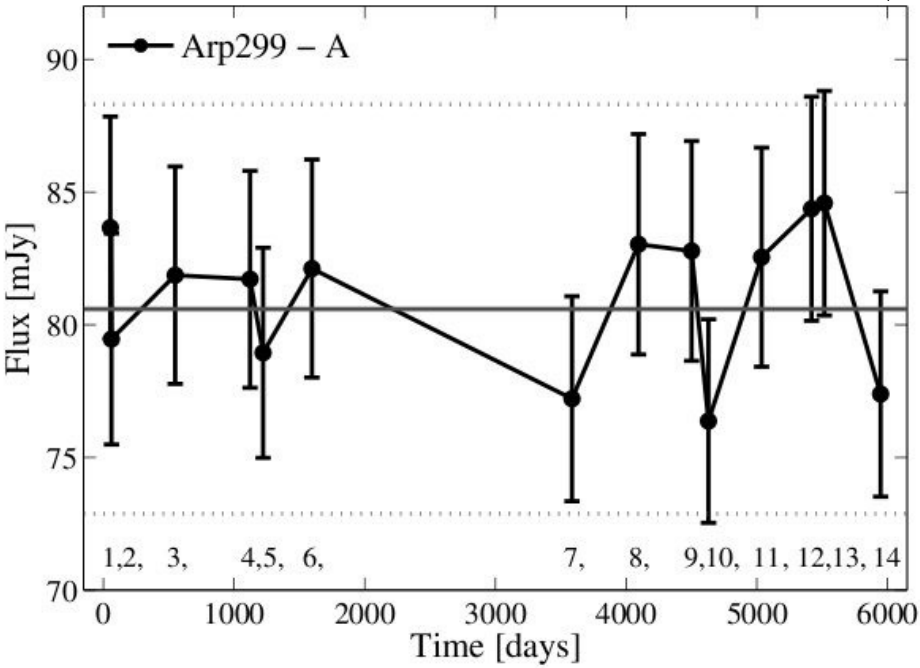
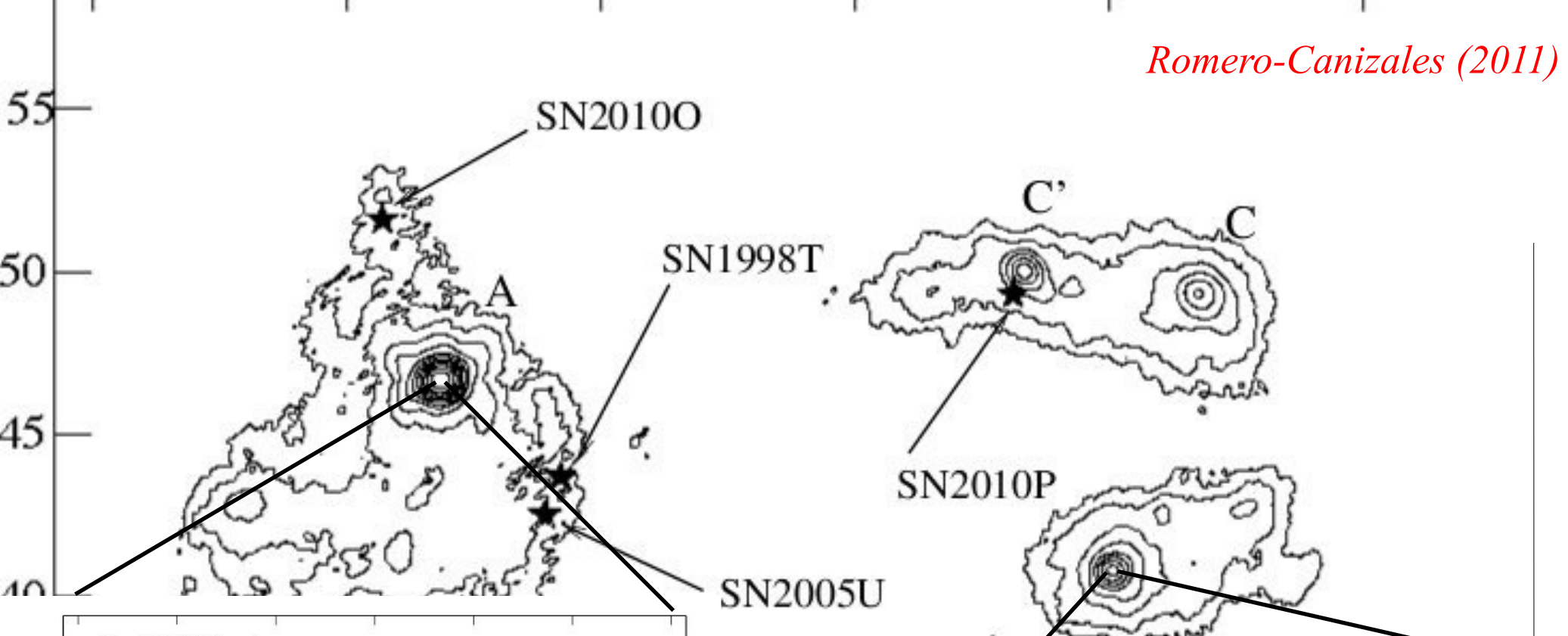
1 kpc

SN1992bu 

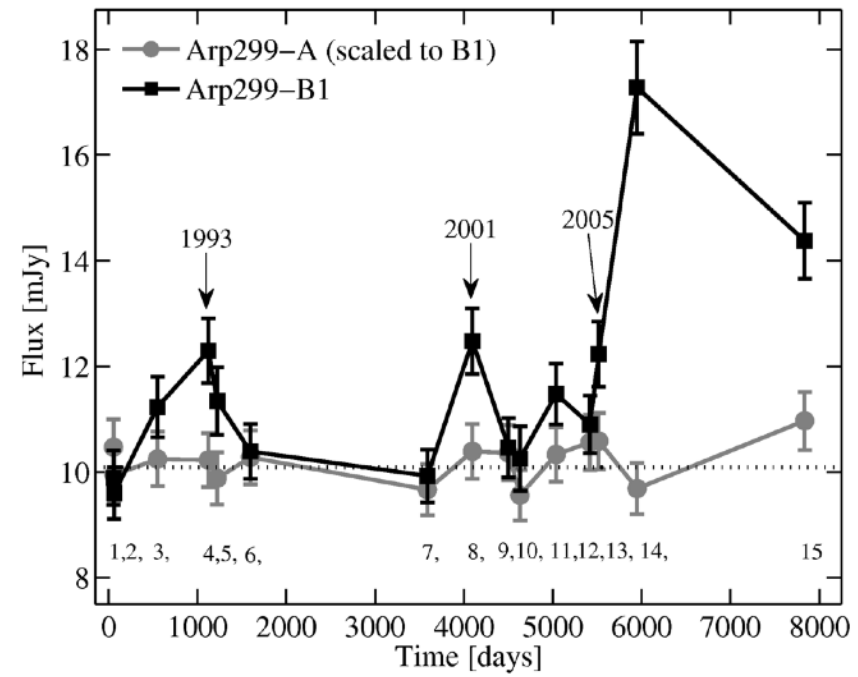
Gemini-N/Altair near-infrared (1.1-2.2 μm) (PSF FWHM $\sim 0.1''$)



Very Large Array (VLA) radio image (8.46 GHz = 3.5 cm) (PSF FWHM ~ 0.5'')

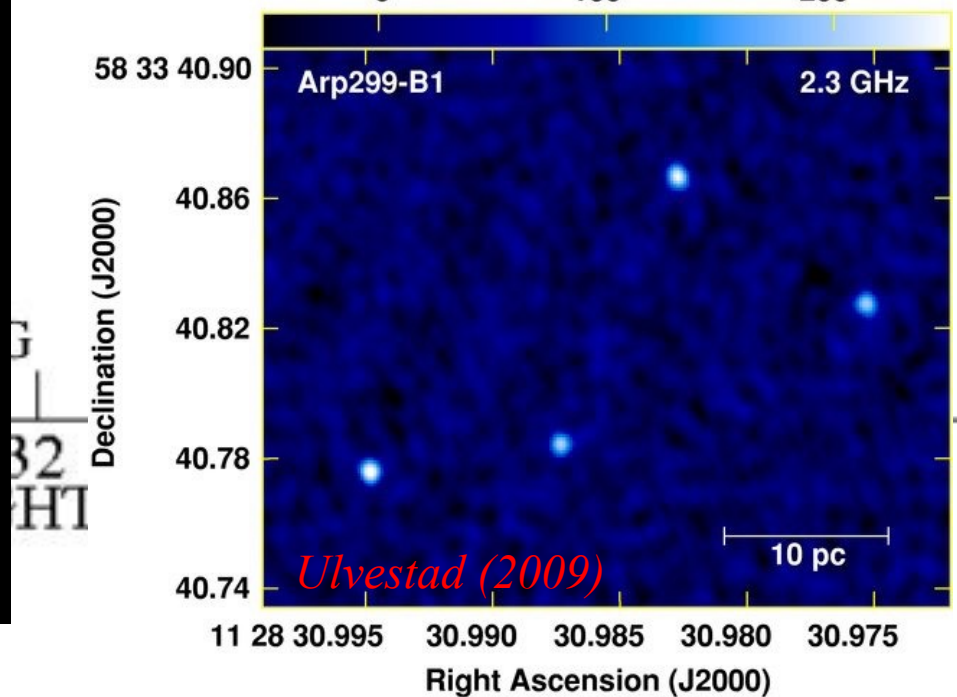
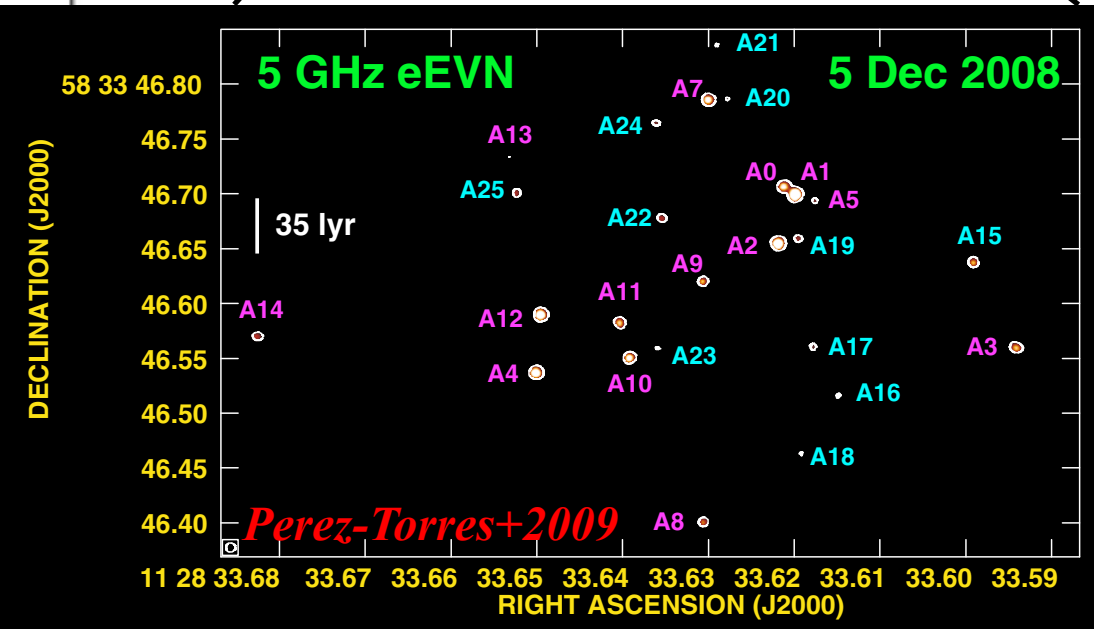
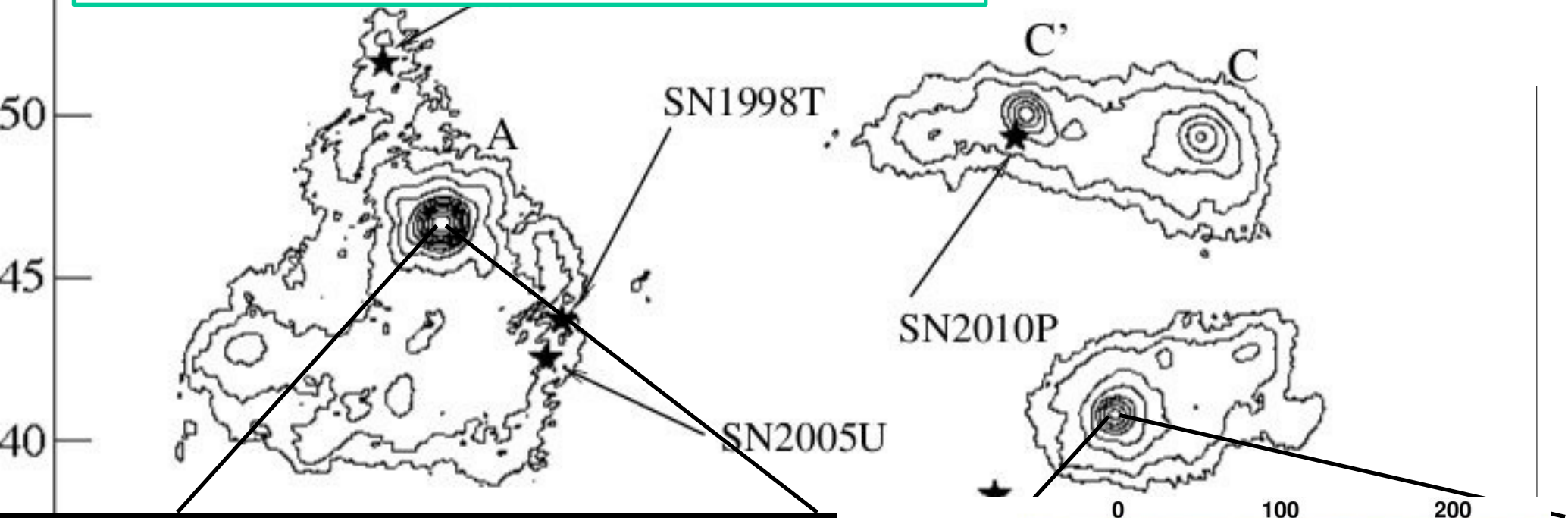


N1993G
32
RIGHT



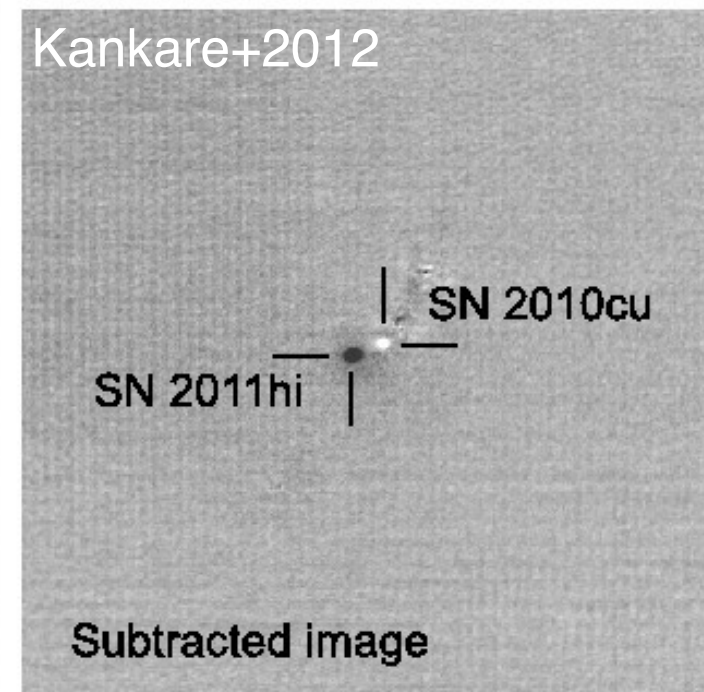
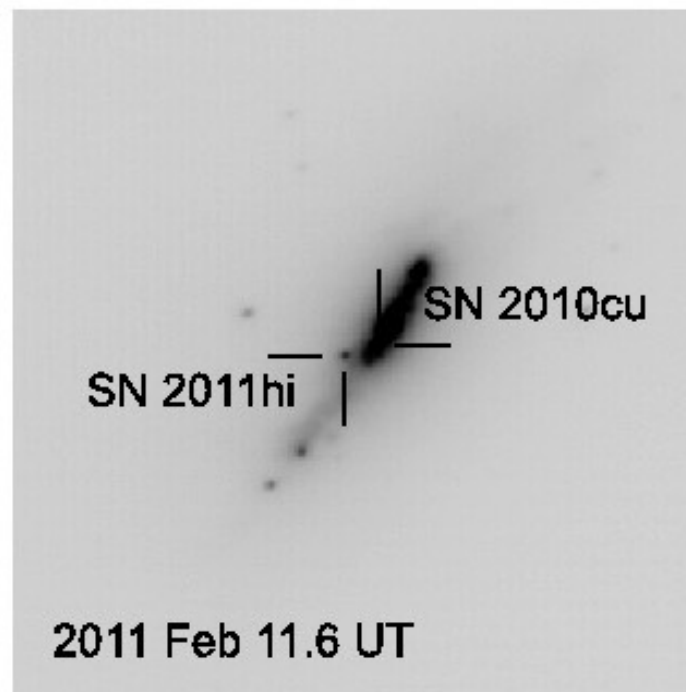
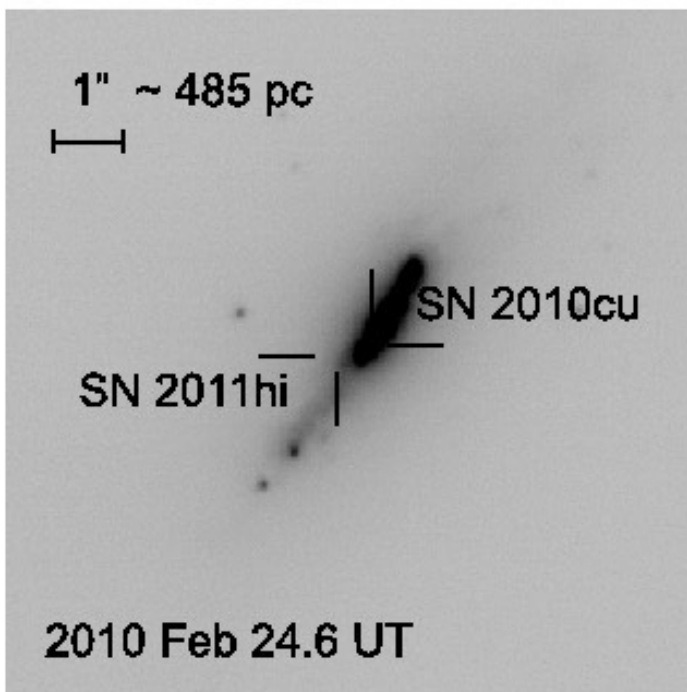
Very Long Baseline Array (VLBA) radio image
(2.3 GHz = 13 cm) PSF FWHM ~ 0.5 milliarcsec

1000 pc



Detecting time-variability: astronomical and medical imaging

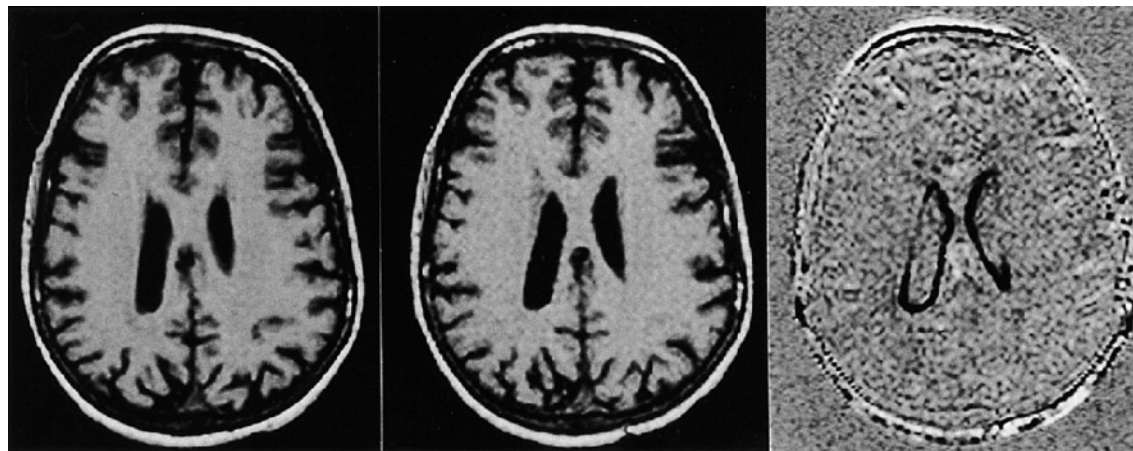
- Detection and study of stellar explosions (supernovae) by repeated imaging of galaxies
 - SN detection by precise image alignment, matching of the point spread functions (PSFs), intensity and background levels followed by image subtraction



Detecting time-variability: astronomical and medical imaging

- Detection and study of stellar explosions (supernovae) by repeated imaging of galaxies
 - SN detection by precise image alignment, matching of the point spread functions (PSFs), intensity and background levels followed by image subtraction
- Monitoring of volumetric changes, e.g., loss of tissue in Alzheimer's
 - Register new and reference images using natural landmarks, normalise image intensities and apply image subtraction to reveal tiny volumetric changes

Reference new +6 months subtracted



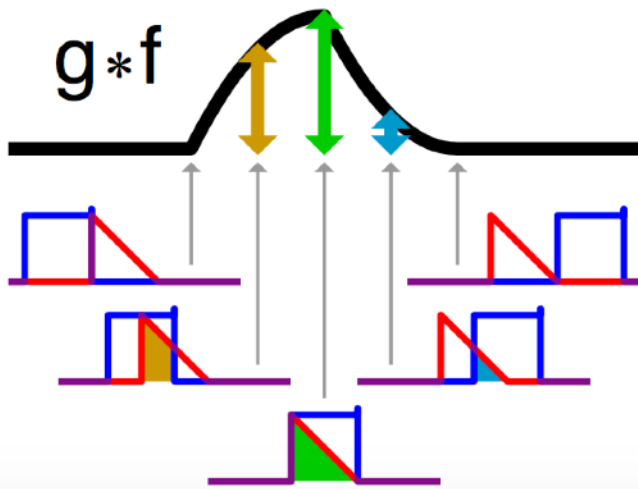
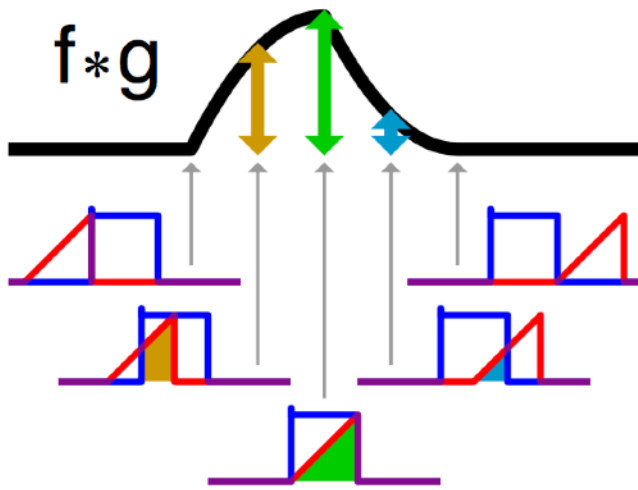
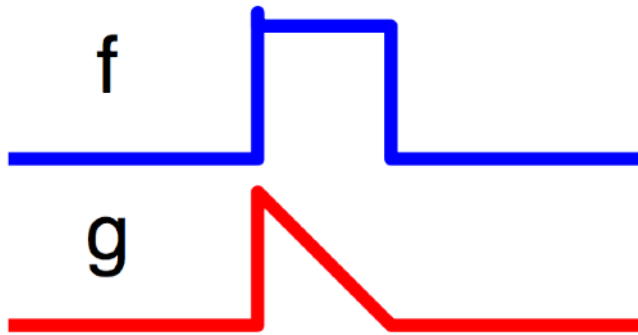
(a)

(b)

(c)

Bradley et al. 2002, British J. of Radiology, 75, 506

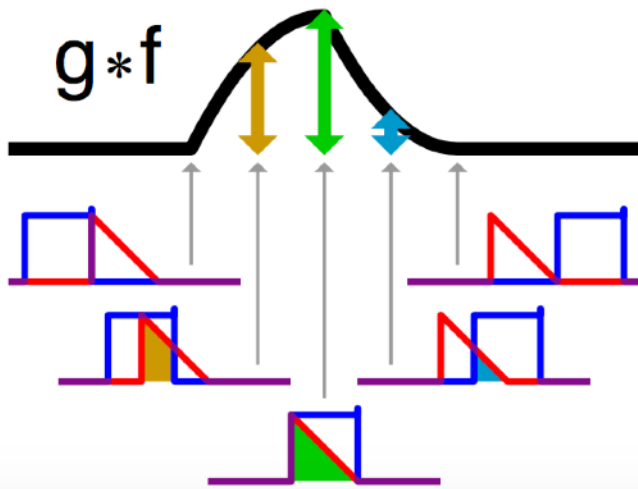
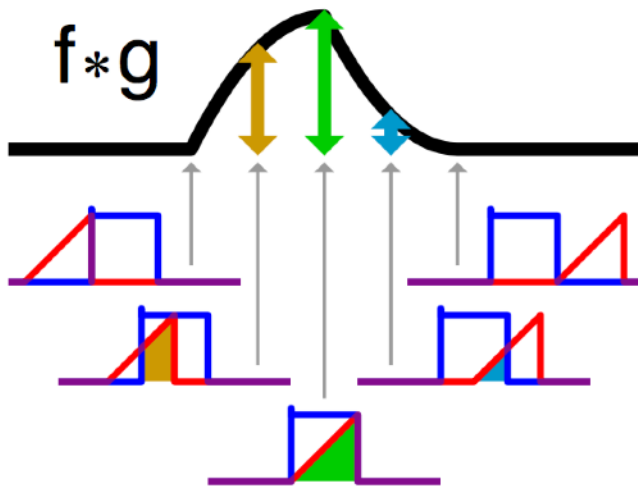
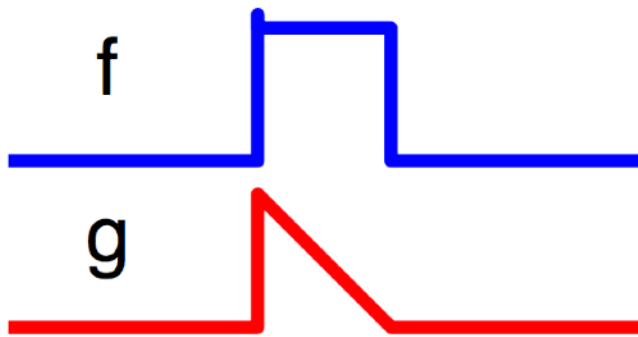
Convolution



$$(f * g)(x) = \int_{-\infty}^{\infty} f(\tau)g(x - \tau) d\tau$$

$$(f * g)_j = \sum_{k=-m/2+1}^{m/2} f_k g_{j-k}$$

Convolution



$$F(u, v) = \text{FT}\{f(x, y)\}$$

i.e.,

$$F(u, v) = \int_{-\infty}^{\infty} \int_{-\infty}^{\infty} f(x, y) \exp[2\pi i(ux + vy)] dx dy$$

Linearity

$$\text{FT}\{f(x, y) + g(x, y)\} = F(u, v) + G(u, v)$$

Convolution

$$\text{FT}\{f(x, y) * g(x, y)\} = F(u, v) \cdot G(u, v)$$

Shift

$$\text{FT}\{f(x - x_i, y - y_i)\} = F(u, v) \exp[2\pi i(ux_i + vy_i)]$$

Similarity

$$\text{FT}\{f(ax, by)\} = \frac{1}{|ab|} F\left(\frac{u}{a}, \frac{v}{b}\right)$$

Convolution

- With convolution can reduce the noise and therefore increase the S/N while degrading spatial resolution

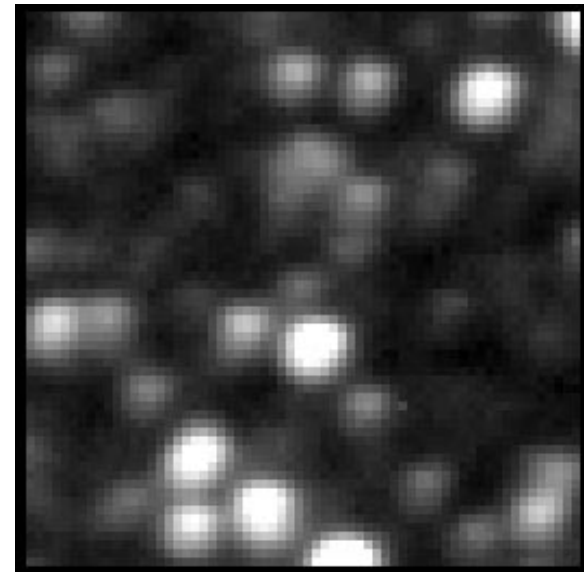
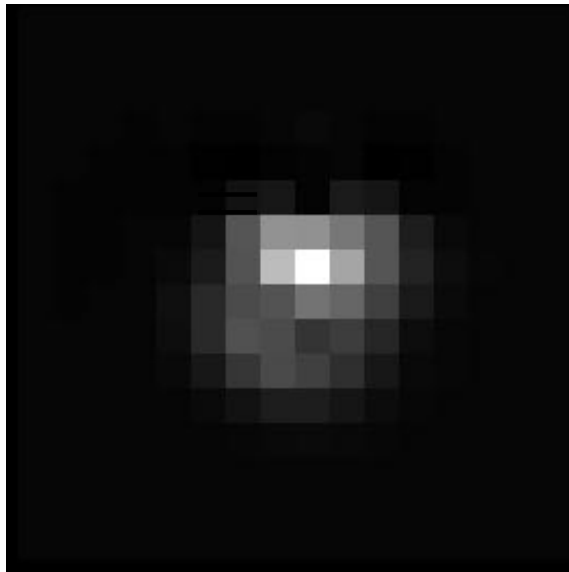
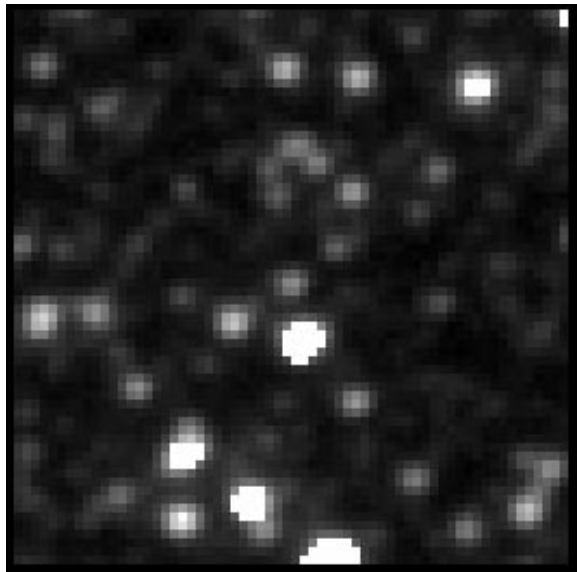
“real” signal

additive noise

$$b(\vec{x}) = f(\vec{x}) * p(\vec{x}) + n(\vec{x})$$

observed signal

PSF



$$ref(x, y) \otimes kernel(x, y, u, v) = im(x, y)$$

Convolution

- With convolution can reduce the noise and therefore increase the S/N while degrading spatial resolution

$$b(\vec{x}) = f(\vec{x}) * p(\vec{x}) + n(\vec{x})$$

“real” signal **additive noise**

observed signal **PSF**

In the case of 1-D functions

$$(f * g)(x) = \int_{-\infty}^{\infty} f(\tau)g(x - \tau) d\tau$$

In the case of discrete 1-D functions

$$(f * g)_j = \sum_{k=-m/2+1}^{m/2} f_k g_{j-k}$$

Deconvolution

We have observed data I (intensity distribution) corresponding to an observation of a “real image” O through an imaging system characterised by the PSF P and additive noise N .

$$\begin{aligned} I(x, y) &= \int_{x_1=-\infty}^{+\infty} \int_{y_1=-\infty}^{+\infty} P(x - x_1, y - y_1) O(x_1, y_1) dx_1 dy_1 \\ &+ N(x, y) \\ &= (P * O)(x, y) + N(x, y), \end{aligned}$$

The Convolution Theorem:
Convolution in either domain is equivalent to multiplication in the other.

In Fourier space:

$$\hat{I}(u, v) = \hat{O}(u, v) \hat{P}(u, v) + \hat{N}(u, v).$$

Starck, Pantin & Murtagh 2002: Deconvolution in Astronomy

<https://iopscience.iop.org/article/10.1086/342606/pdf>

Deconvolution

In Fourier space:

$$\hat{I}(u, v) = \hat{O}(u, v)\hat{P}(u, v) + \hat{N}(u, v).$$

$$\frac{\hat{I}(u, v)}{\hat{P}(u, v)} = \hat{O}(u, v) + \frac{\hat{N}(u, v)}{\hat{P}(u, v)}.$$

This method, sometimes called the *Fourier-quotient method*, is very fast. We need to do only a Fourier transform and an inverse Fourier transform. However, in the presence of noise, this method cannot be used.

Difference imaging in astronomy



Sep, 1994



Mar, 1995



Feb, 1996



Jul, 1997



Feb, 1998



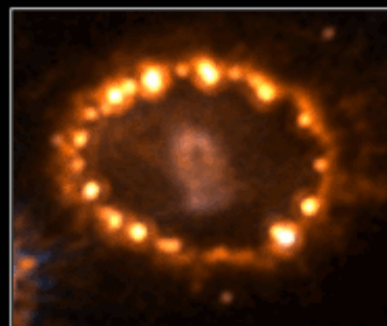
Apr, 1999



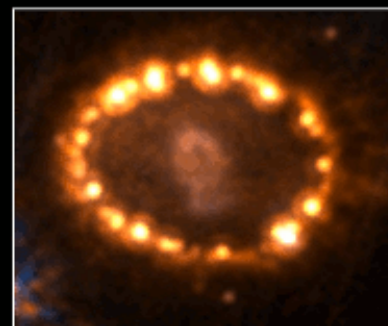
Nov, 2000



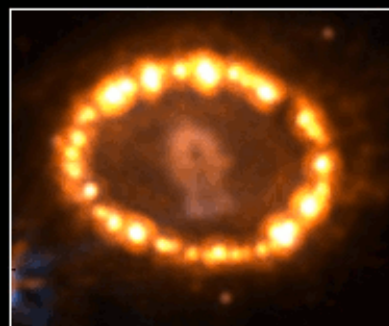
Dec, 2001



Jan, 2003



Nov, 2003



Sep, 2005



Apr, 2006



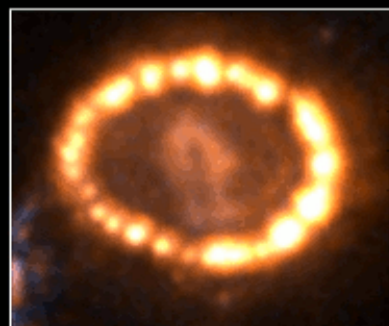
Dec, 2006



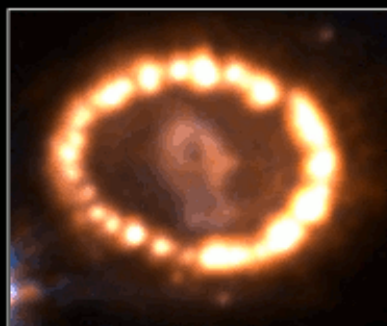
May, 2007



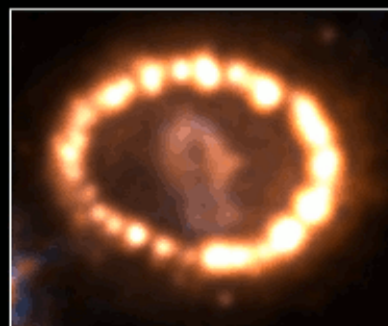
Feb, 2008



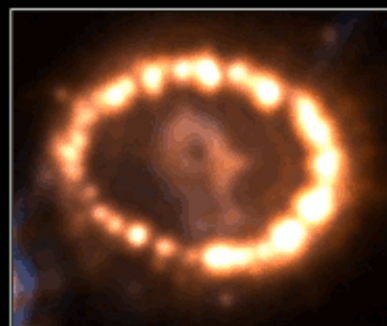
Apr, 2009



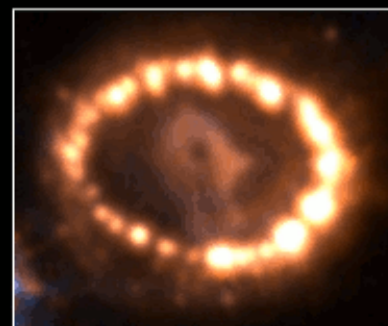
Dec, 2009



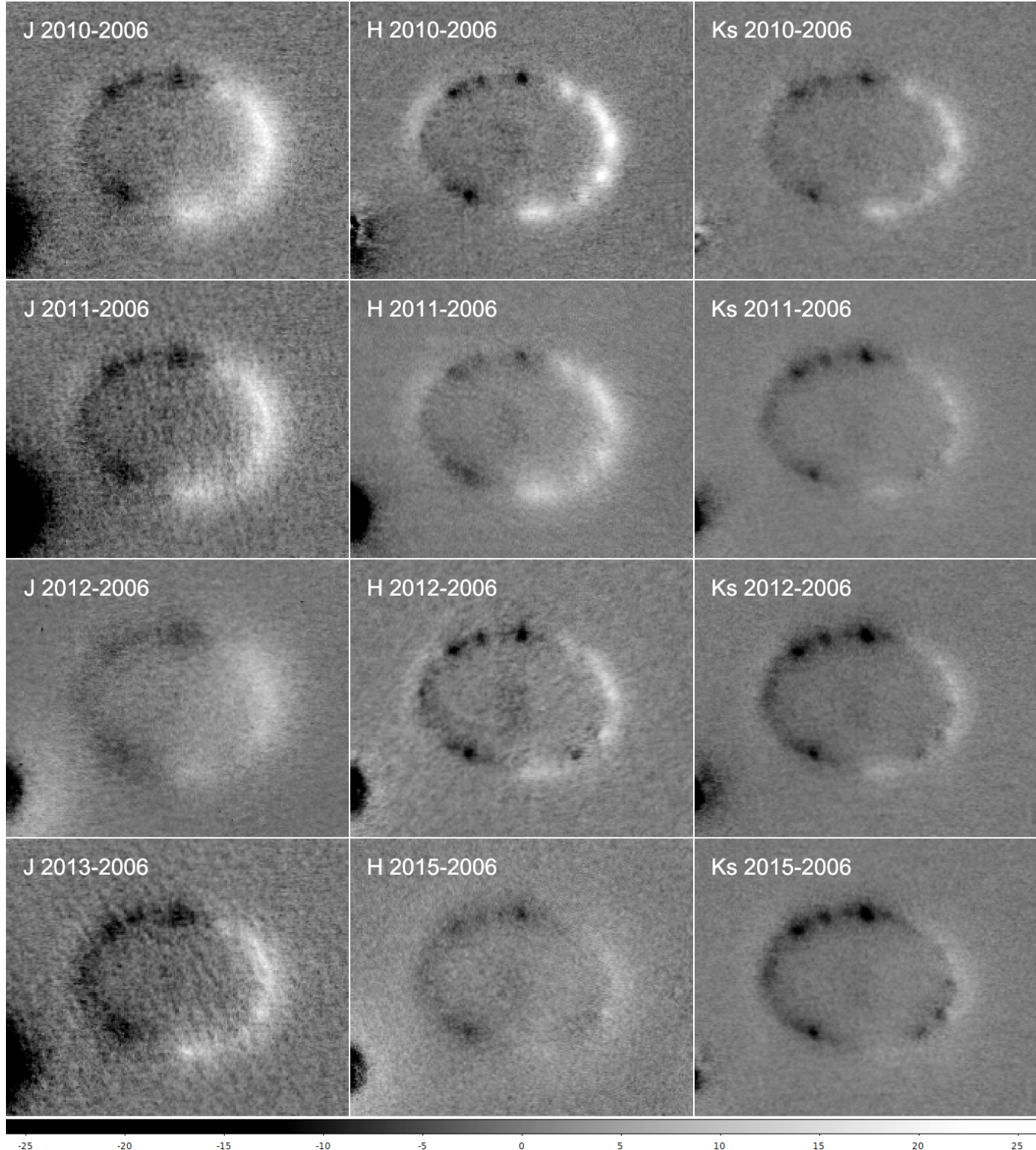
Jan, 2011



Feb, 2013



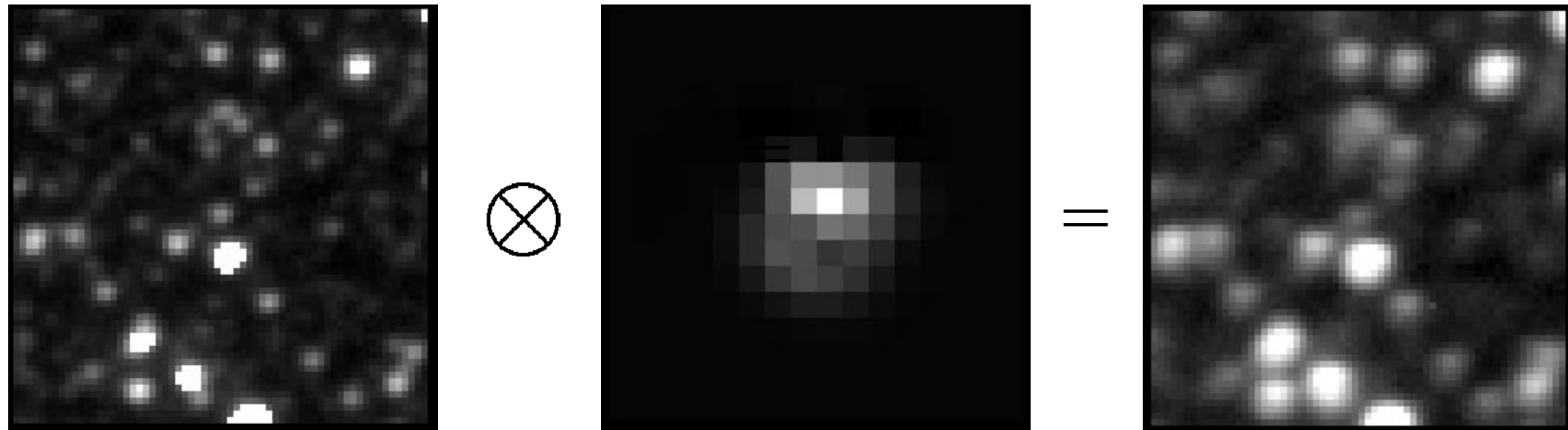
Jun, 2014



Ahola (2018)

Optimal Image Subtraction

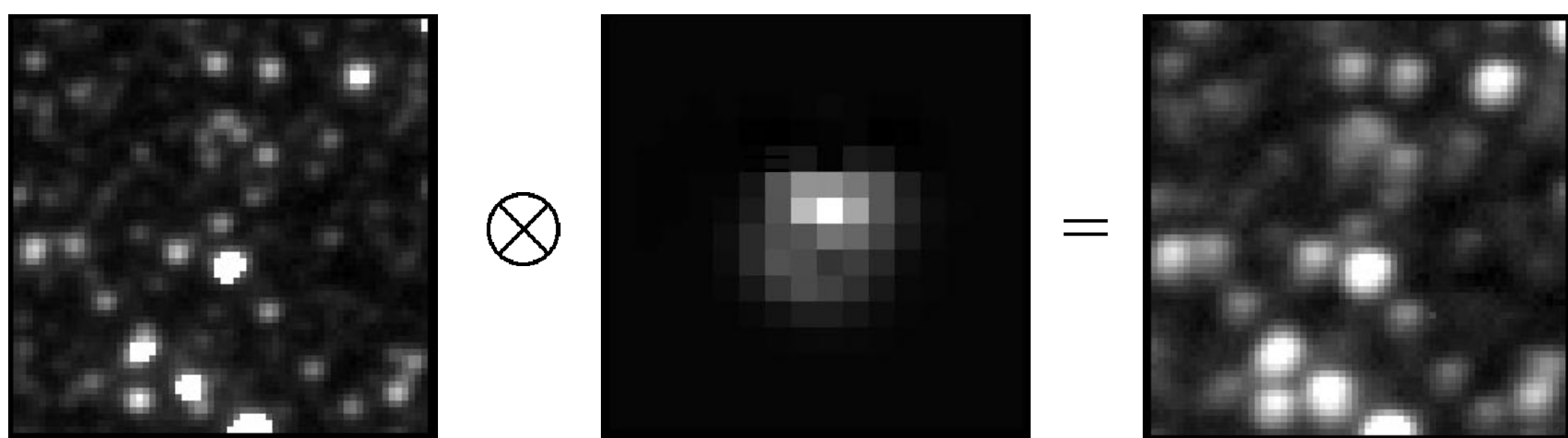
$$ref(x, y) \otimes kernel(x, y, u, v) = im(x, y) + bg(x, y)$$



Optimal Image Subtraction

$$ref(x, y) \otimes kernel(x, y, u, v) = im(x, y) + bg(x, y)$$

$$kernel(x, y, u, v) = \sum_n \sum_{d_n^x} \sum_{d_n^y} \sum_{\delta^x} \sum_{\delta^y} [a_n \underbrace{x^{\delta^x} y^{\delta^y}}_3 \underbrace{e^{-(u^2+v^2)/2\sigma_n^2}}_1 \underbrace{u^{d_n^x} v^{d_n^y}}_2]$$

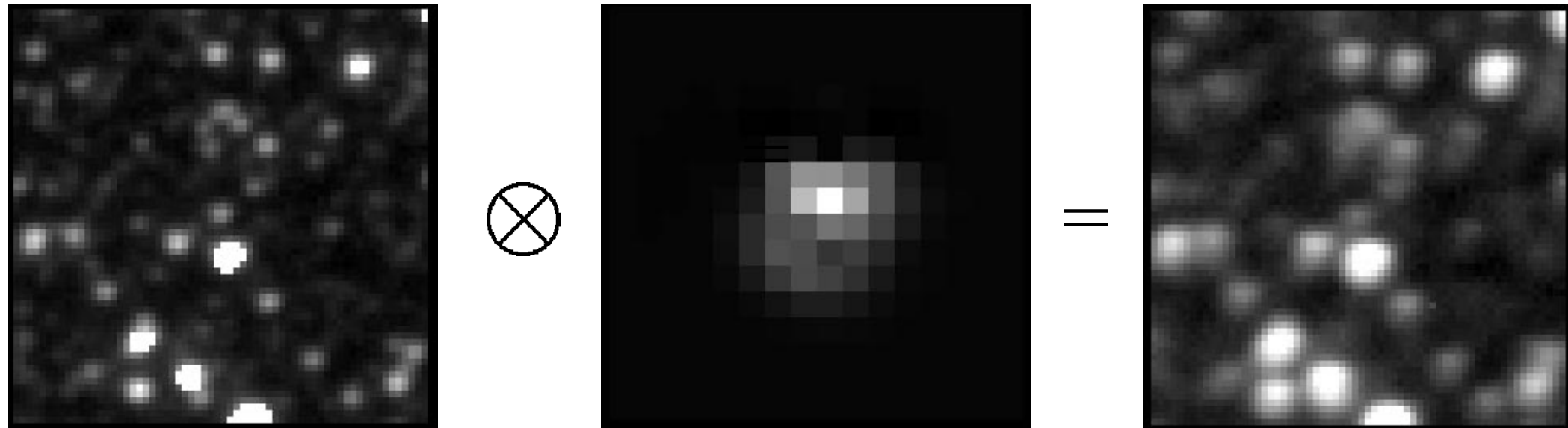


Optimal Image Subtraction

$$ref(x, y) \otimes kernel(x, y, u, v) = im(x, y) + bg(x, y)$$

$$kernel(x, y, u, v) = \sum_n \sum_{d_n^x} \sum_{d_n^y} \sum_{\delta^x} \sum_{\delta^y} [a_n \underbrace{x^{\delta^x} y^{\delta^y}}_3 \underbrace{e^{-(u^2+v^2)/2\sigma_n^2}}_1 \underbrace{u^{d_n^x} v^{d_n^y}}_2]$$

The convolution kernel consists of a set of Gaussian functions (1) which are modified by polynomials (2) and a model for the spatial variations of the kernel (3) where $0 < d_n^y + d_n^x \leq D_n$, and $0 < \delta^y + \delta^x \leq D^k$.

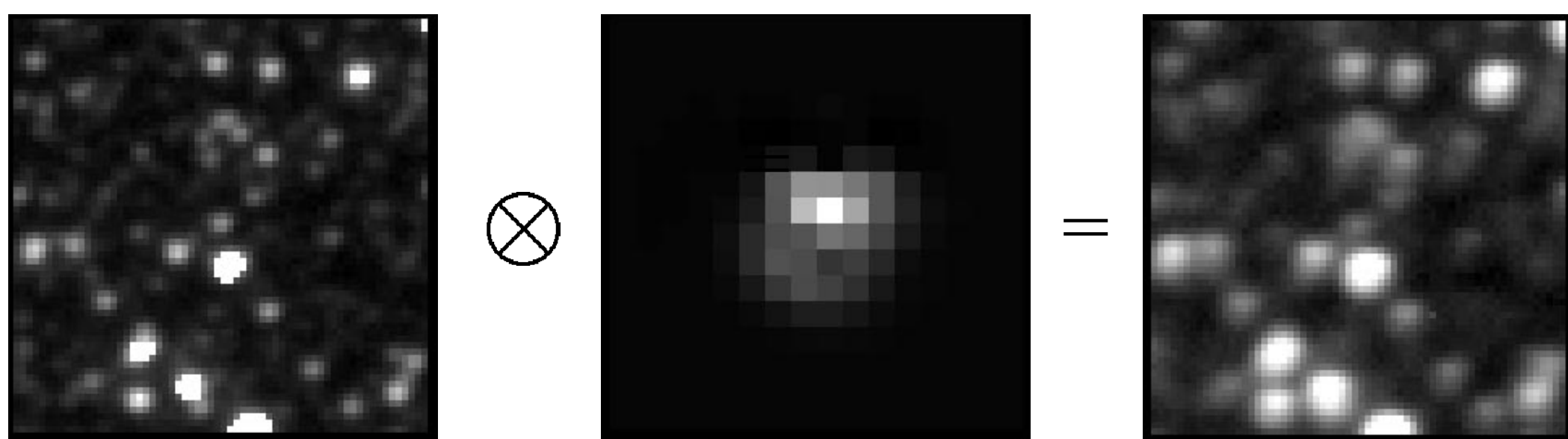


Optimal Image Subtraction

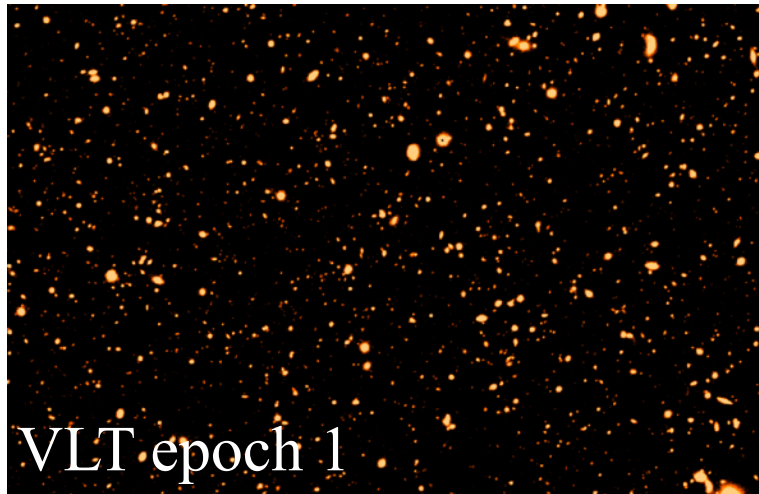
$$ref(x, y) \otimes kernel(x, y, u, v) = im(x, y) + bg(x, y)$$

$$kernel(x, y, u, v) = \sum_n \sum_{d_n^x} \sum_{d_n^y} \sum_{\delta^x} \sum_{\delta^y} [a_n \underbrace{x^{\delta^x} y^{\delta^y}}_3 \underbrace{e^{-(u^2+v^2)/2\sigma_n^2}}_1 \underbrace{u^{d_n^x} v^{d_n^y}}_2]$$

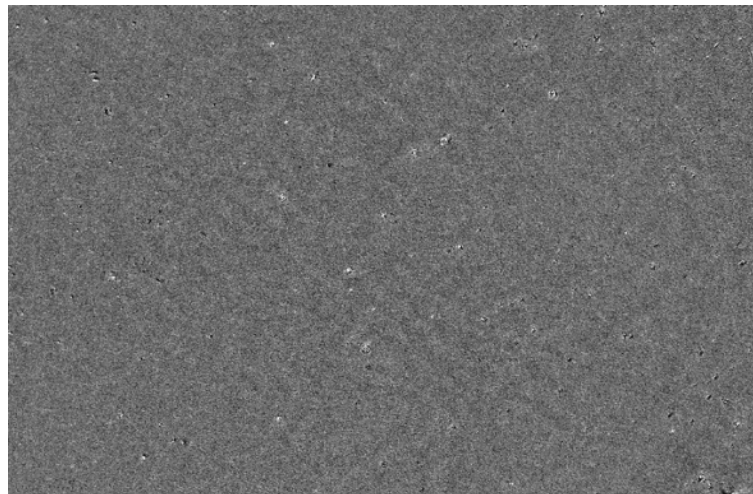
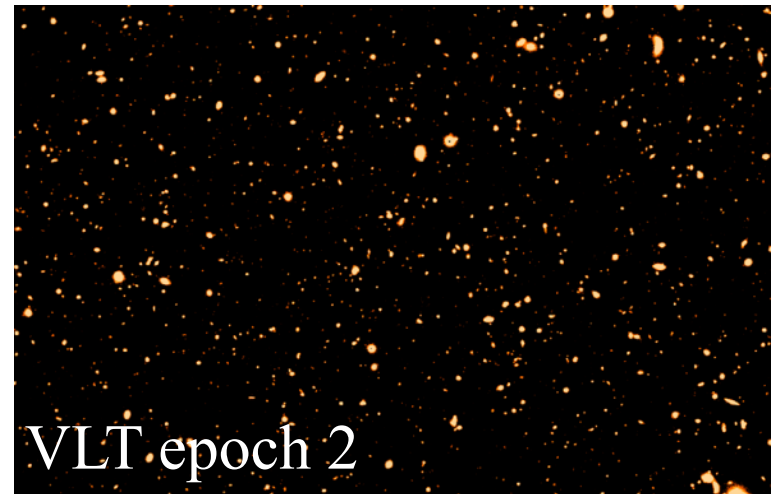
$$bg(x, y) = \sum_i \sum_j a_i x^i y^j$$



Discovery of new astrophysical transients by precise alignment, PSF matching and subtraction of images



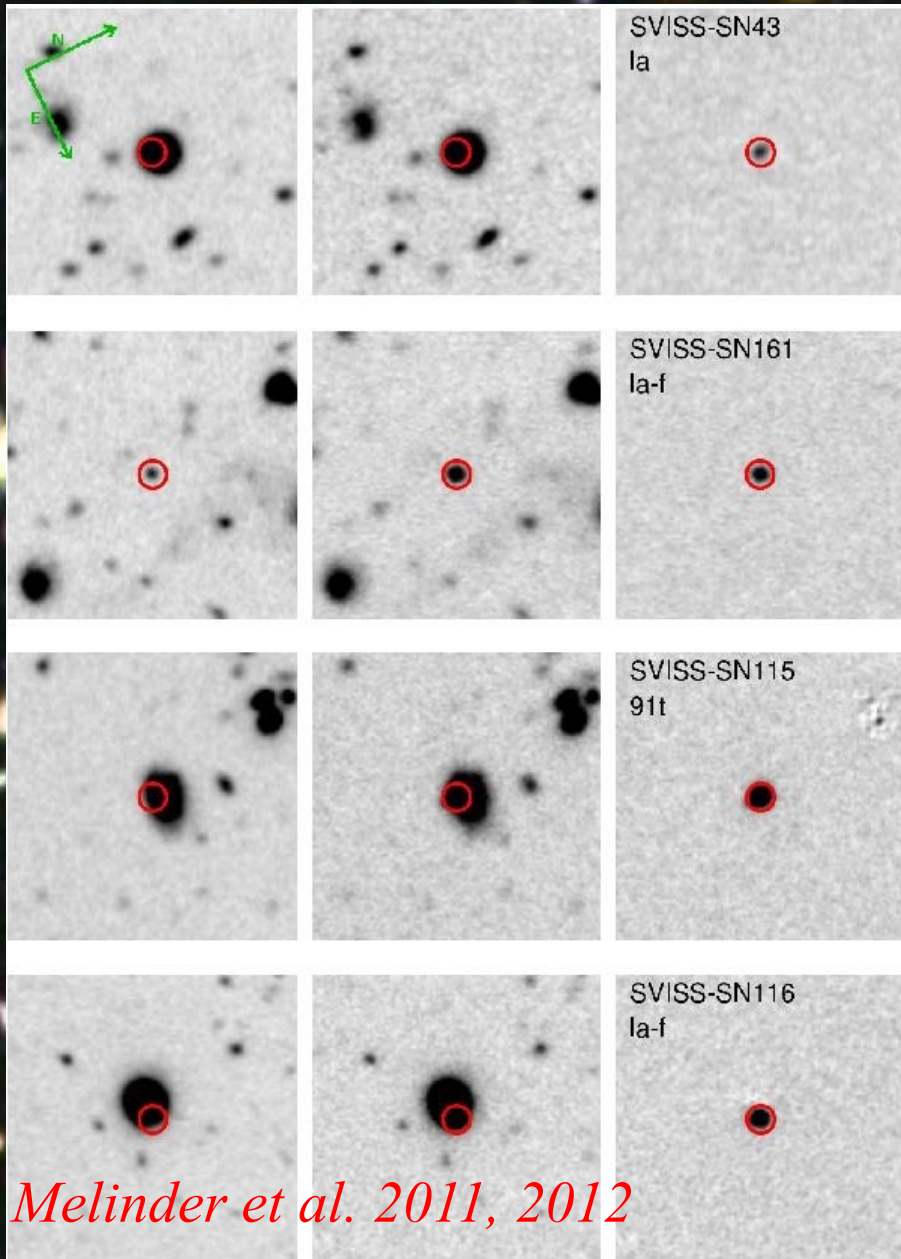
—



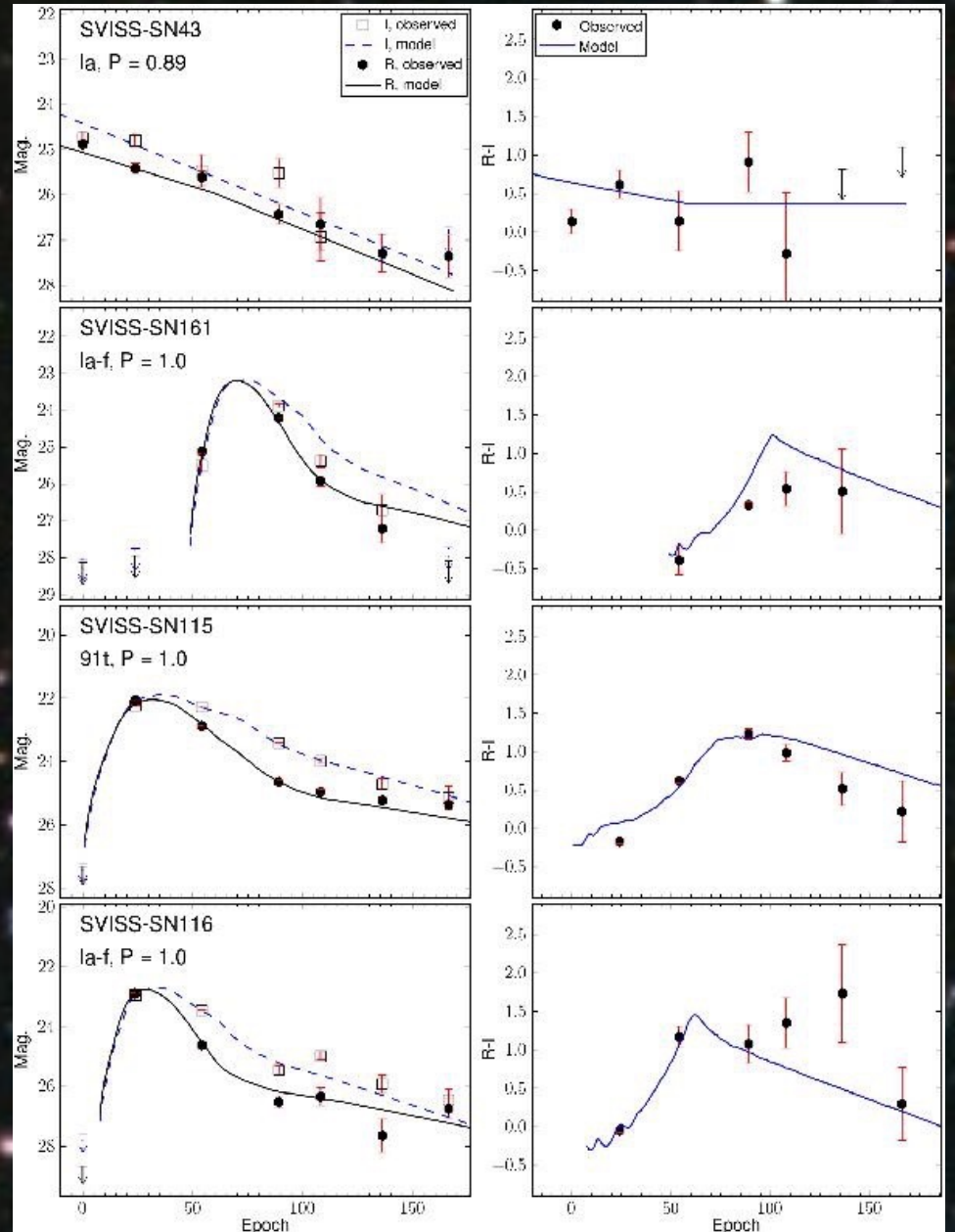


VLT/VIMOS
B 10 hours
V 5 hours
R 15 hours
I 30 hours

Melinder et al. 2011, 2012



Melinder et al. 2011, 2012



Examples of deconvolution

Application of the Richardson-Lucy algorithm in astronomy

THE ASTRONOMICAL JOURNAL

VOLUME 79, NUMBER 6

JUNE 1974

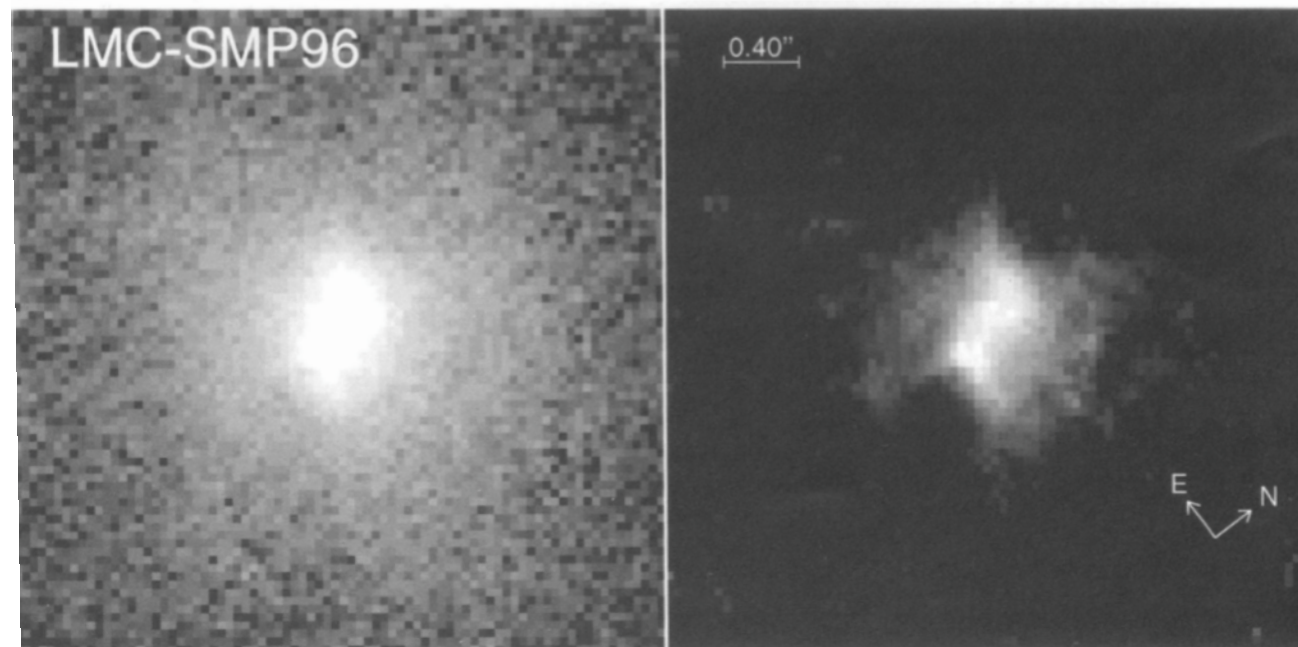
An iterative technique for the rectification of observed distributions

L. B. Lucy*

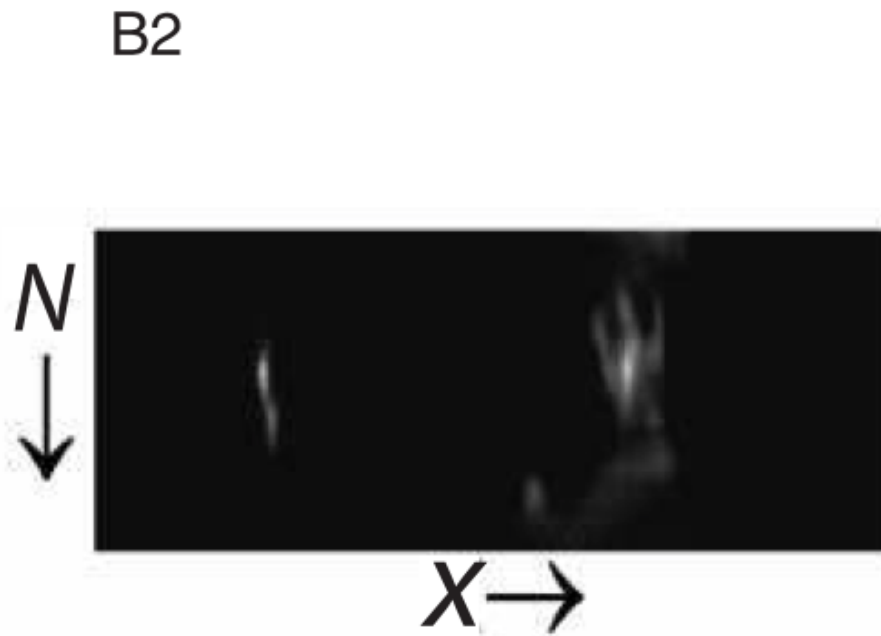
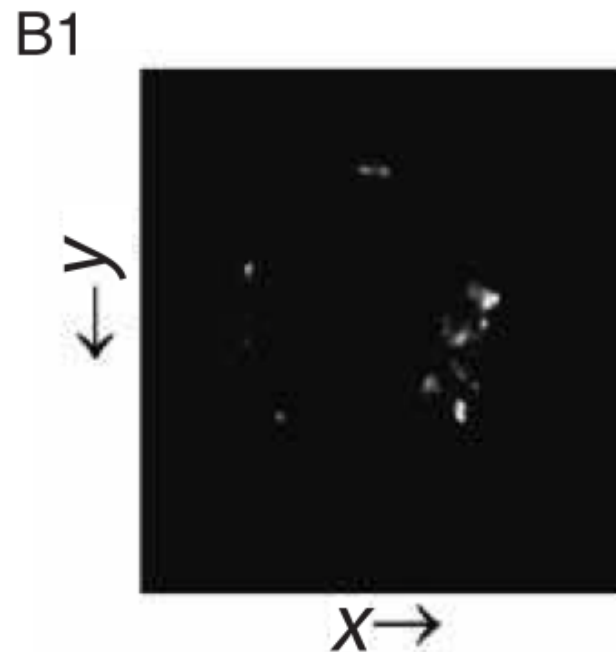
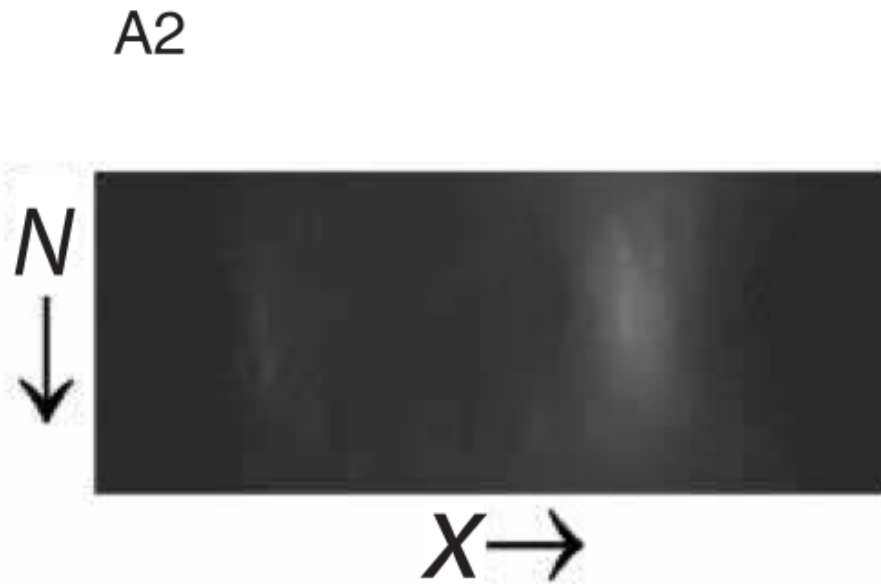
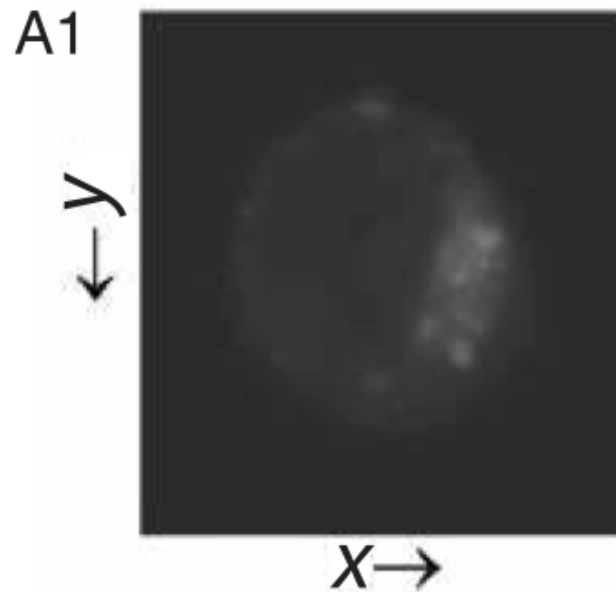
Departments of Physics and Astronomy, The University of Pittsburgh, Pittsburgh, Pennsylvania 15213

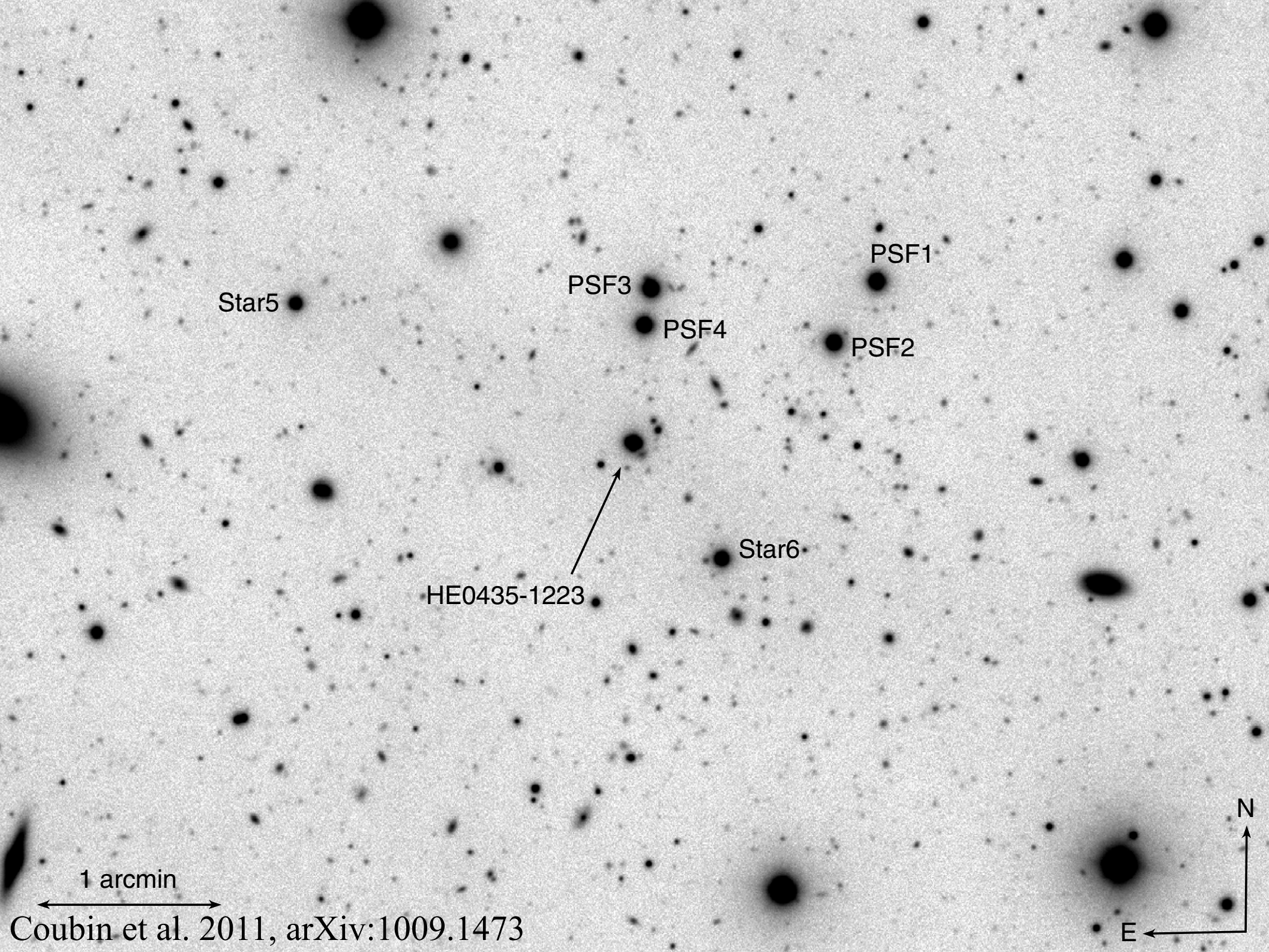
(Received 15 January 1974; revised 26 March 1974)

An iterative technique is described for generating estimates to the solutions of rectification and deconvolution problems in statistical astronomy. The technique, which derives from Bayes' theorem on conditional probabilities, conserves the constraints on frequency distributions (i.e., normalization and non-negativeness) and, at each iteration, increases the likelihood of the observed sample. The behavior of the technique is explored by applying it to problems whose solutions are known in the limit of infinite sample size, and excellent results are obtained after a few iterations. The astronomical use of the technique is illustrated by applying it to the problem of rectifying distributions of $\nu \sin i$ for aspect effect; calculations are also reported illustrating the technique's possible use for correcting radio-astronomical observations for beam-smoothing. Application to the problem of obtaining unbiased, smoothed histograms is also suggested.



Application of the Richardson-Lucy algorithm to medical images





Star5

PSF3

PSF4

PSF1

PSF2

Star6

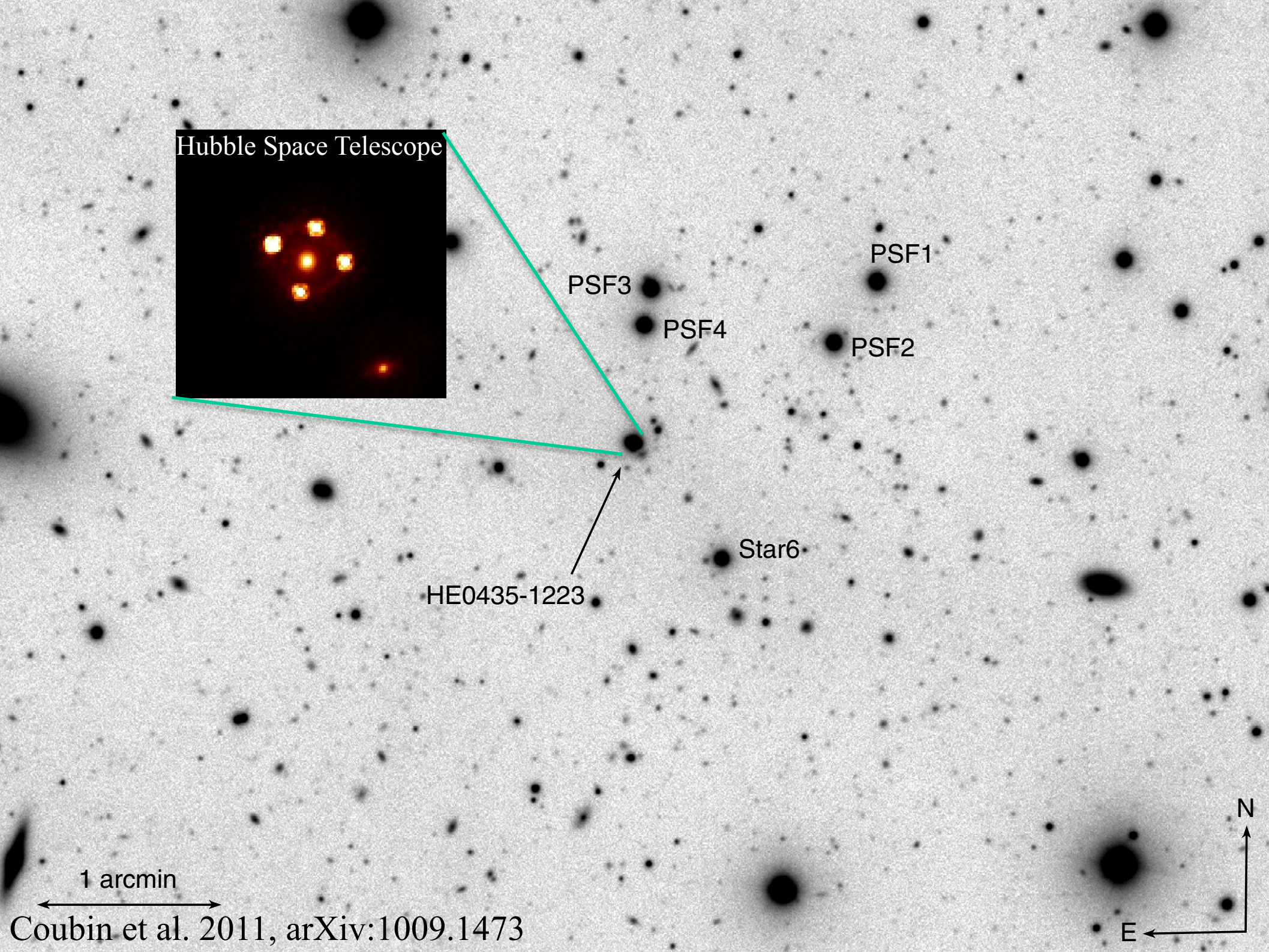
HE0435-1223

1 arcmin

Coubin et al. 2011, arXiv:1009.1473

N

E



Hubble Space Telescope

PSF1

PSF3

PSF4

PSF2

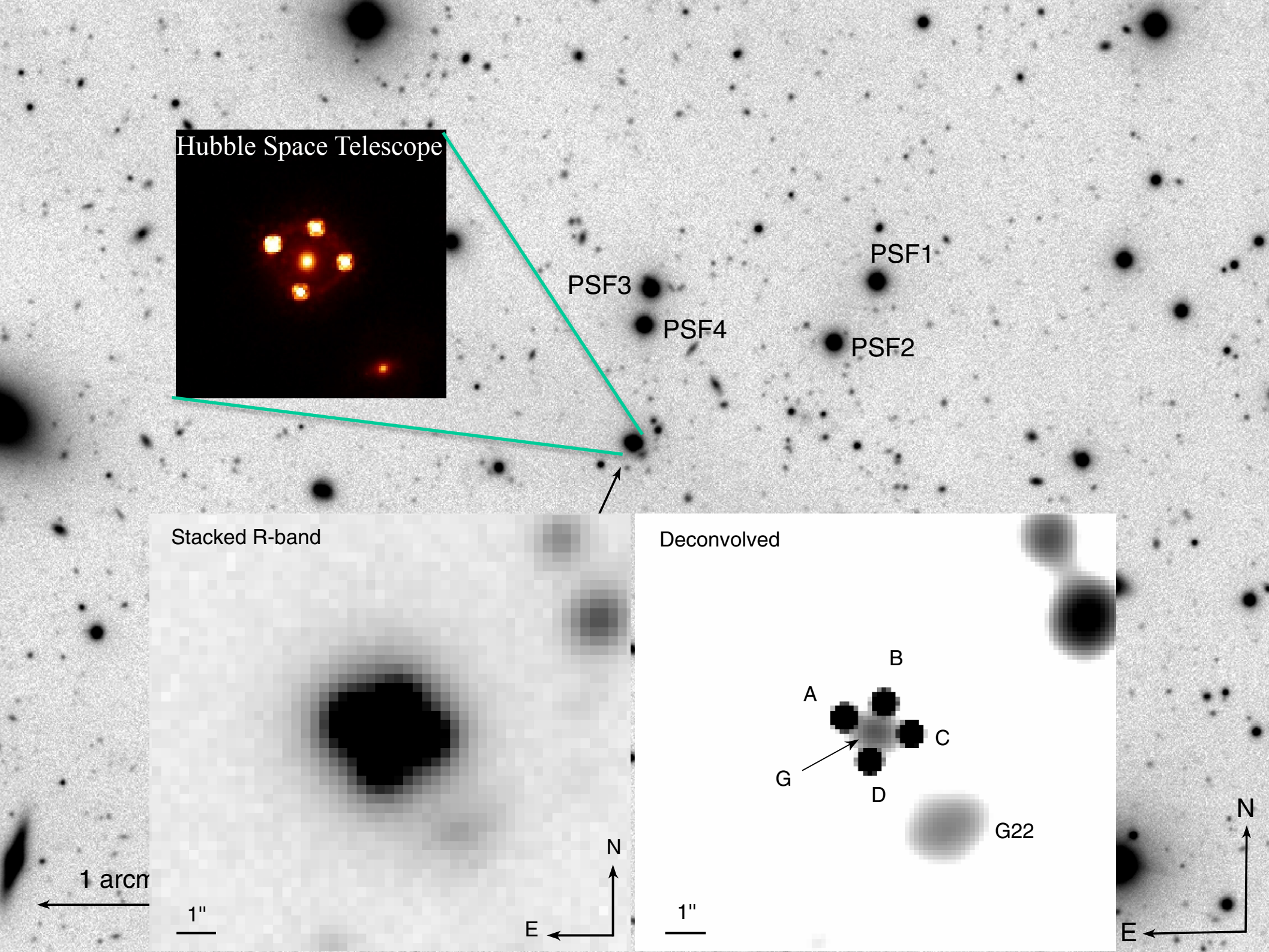
Star6

HE0435-1223

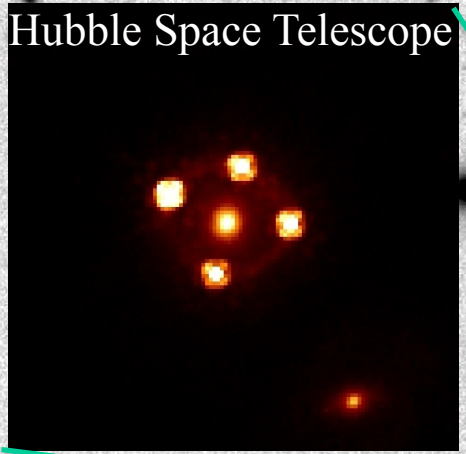
1 arcmin

N

E



Hubble Space Telescope



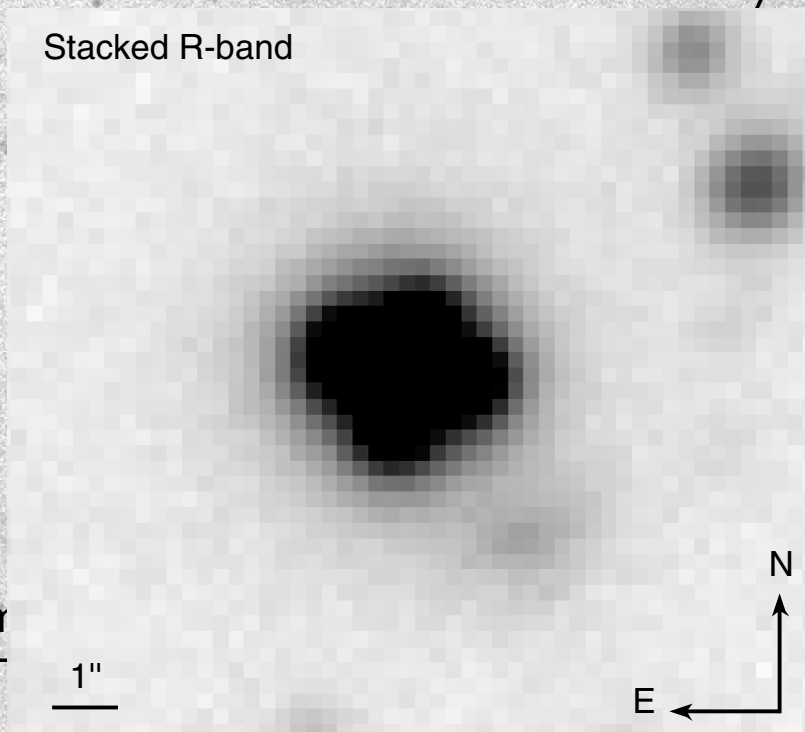
PSF3

PSF4

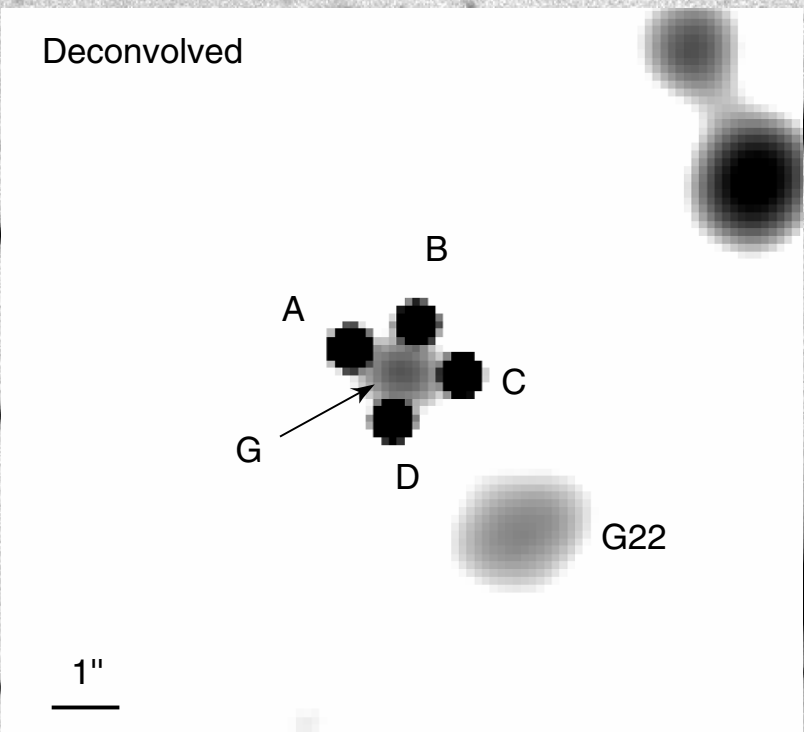
PSF1

PSF2

Stacked R-band



Deconvolved



1 arcmin

1"

E

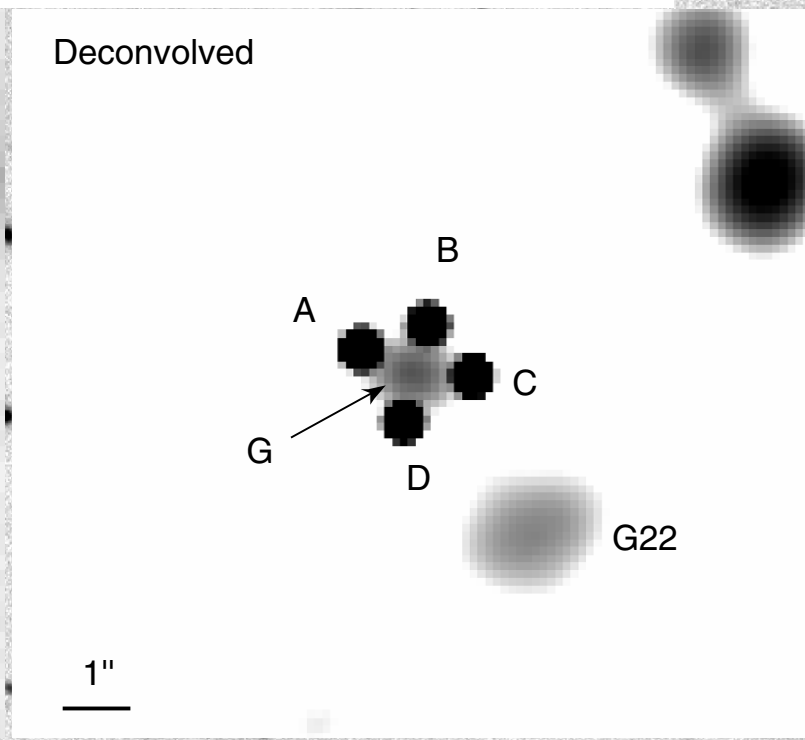
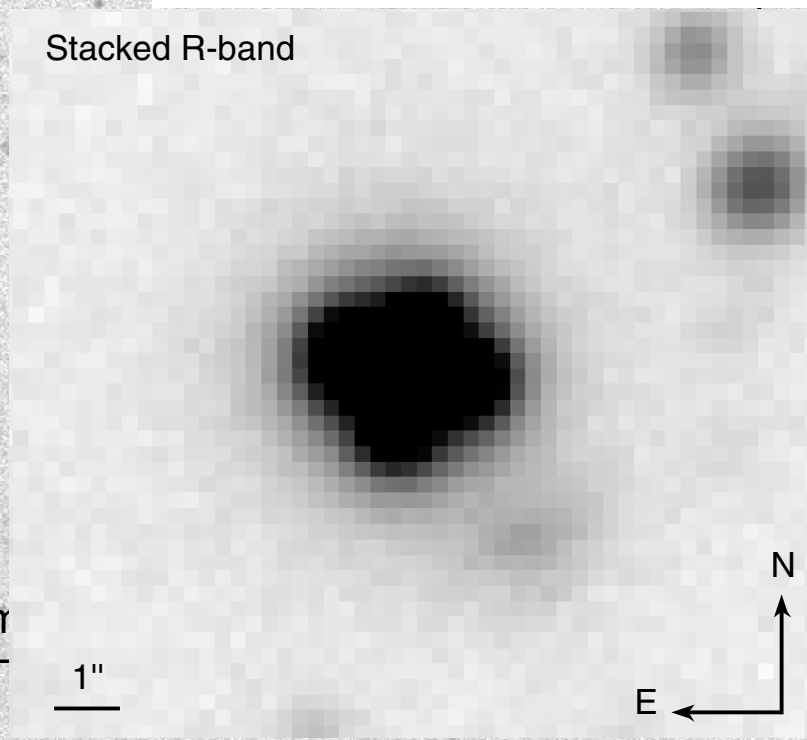
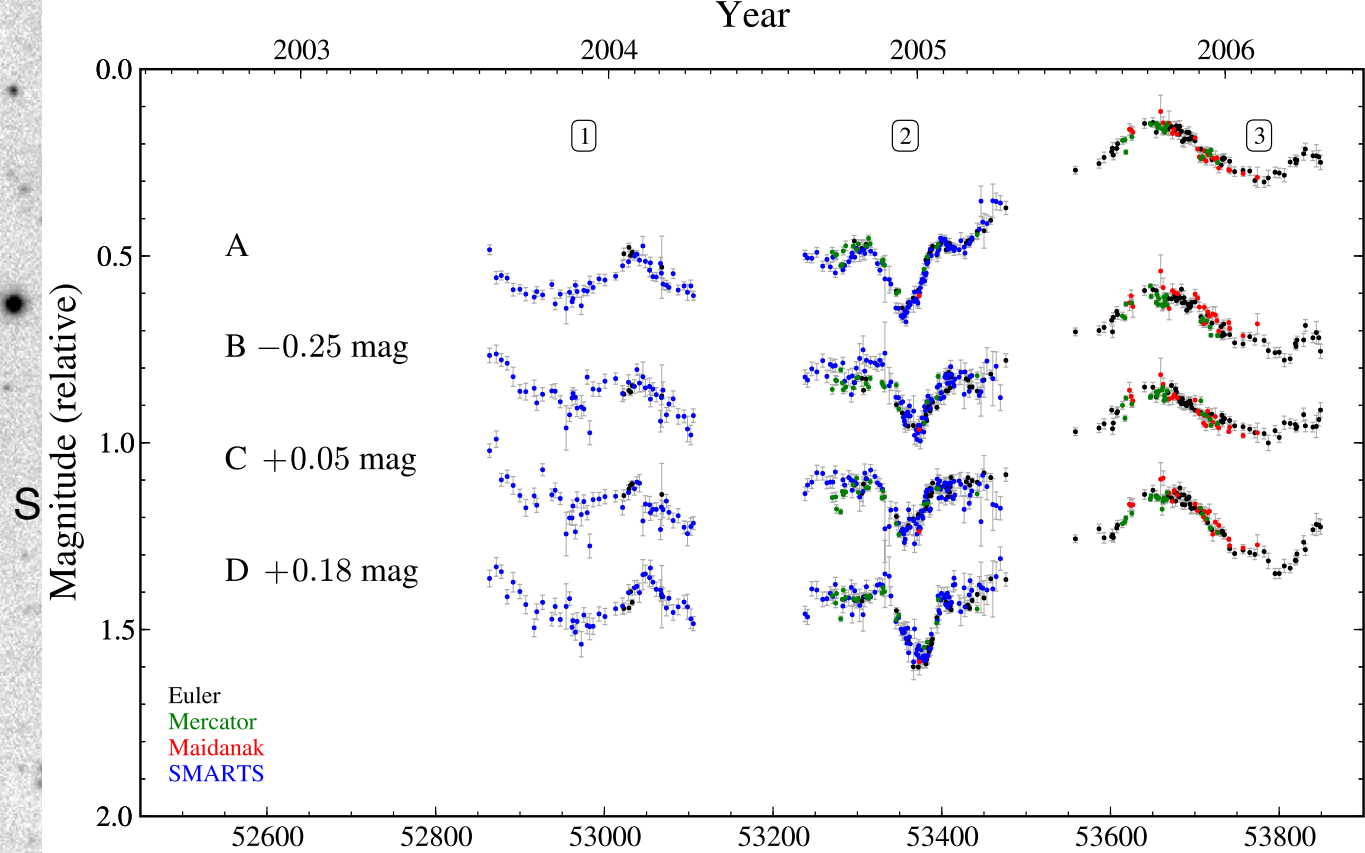
N

1"

G22

E

N



Adaptive optics (AO) imaging

Davies R. 2012: Adaptive Optics for Astronomy
<https://arxiv.org/pdf/1201.5741.pdf>

Adaptive Optics imaging

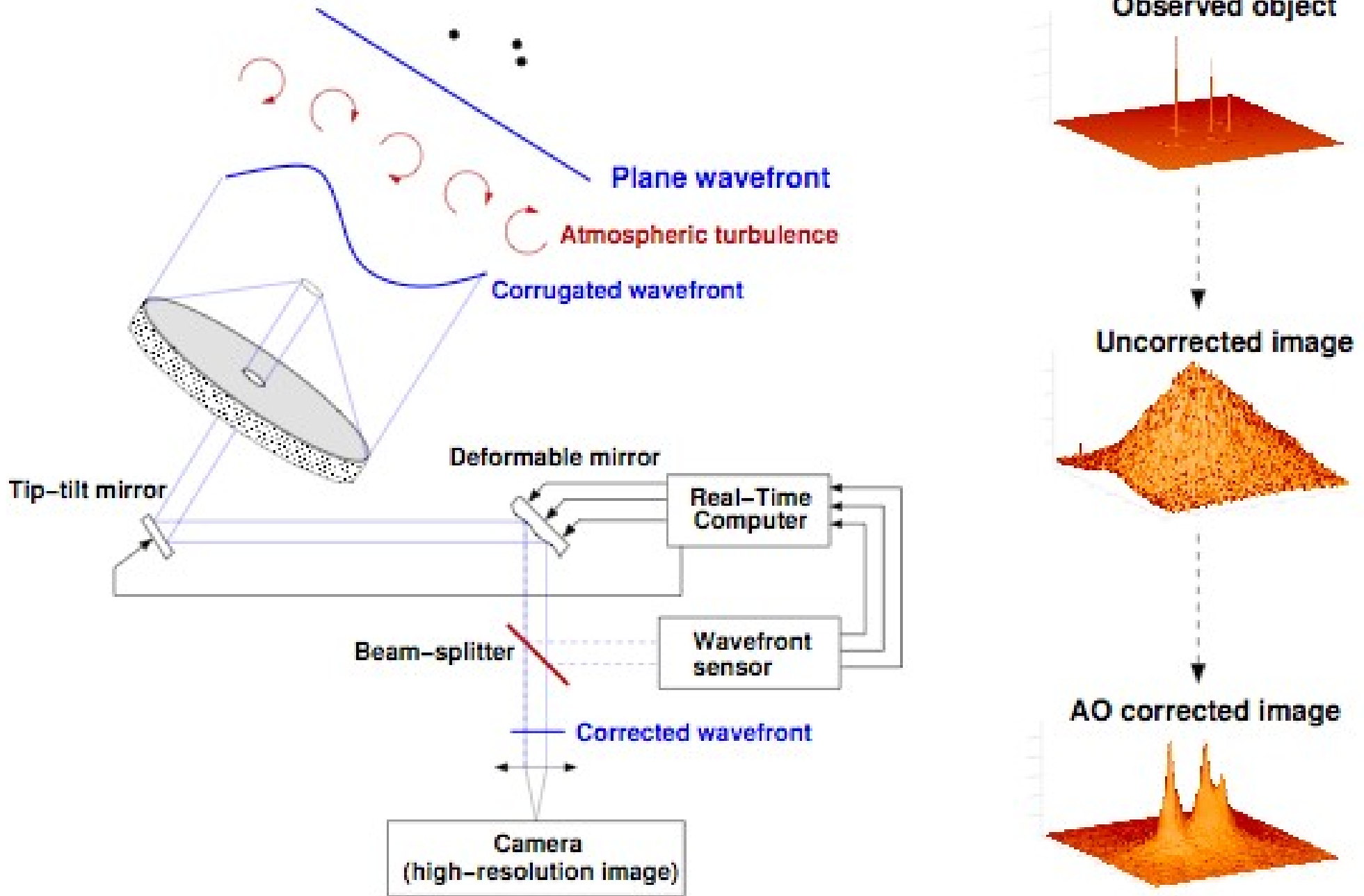
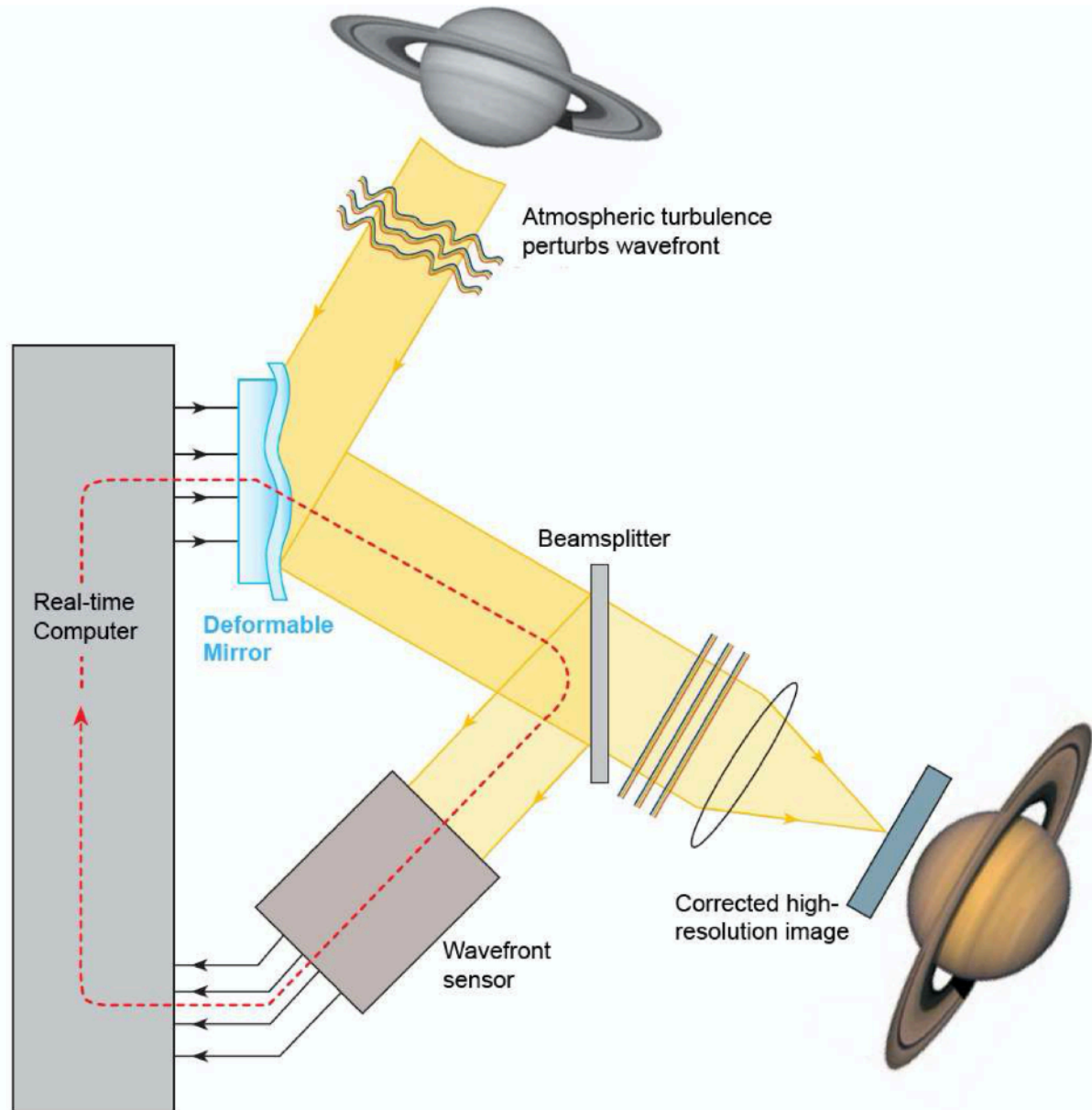
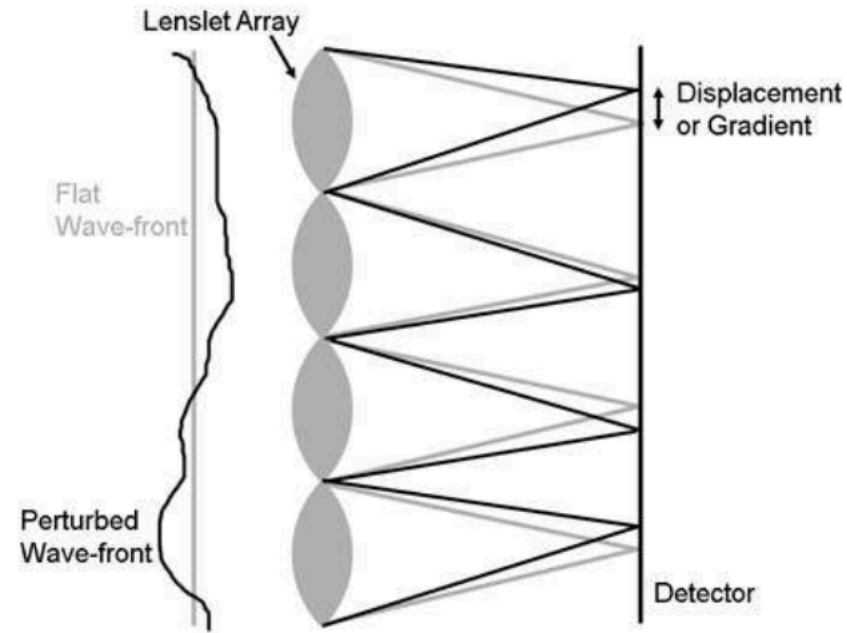


Figure 3-1: Principle of Adaptive Optics

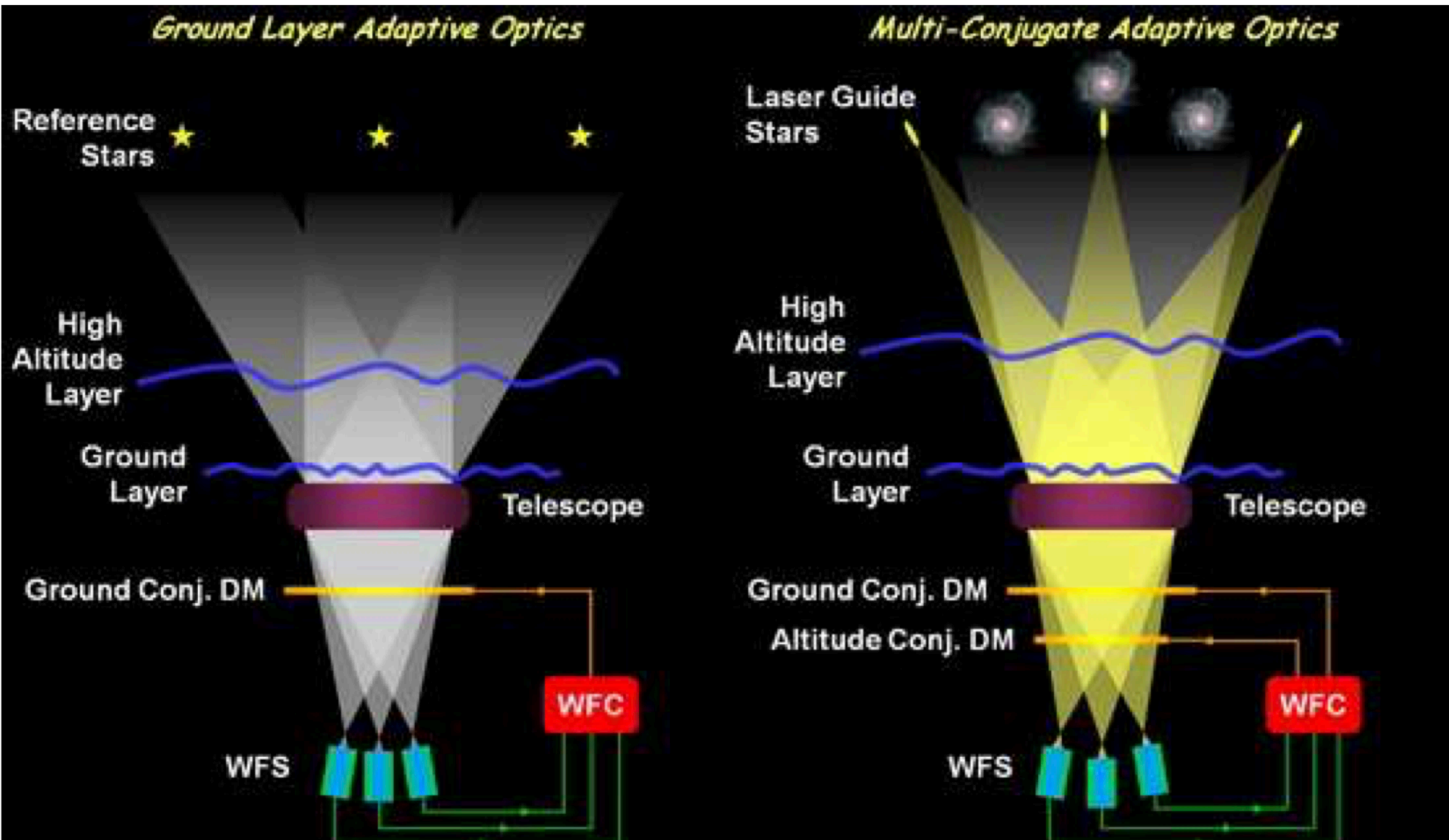
The principles of Adaptive Optics

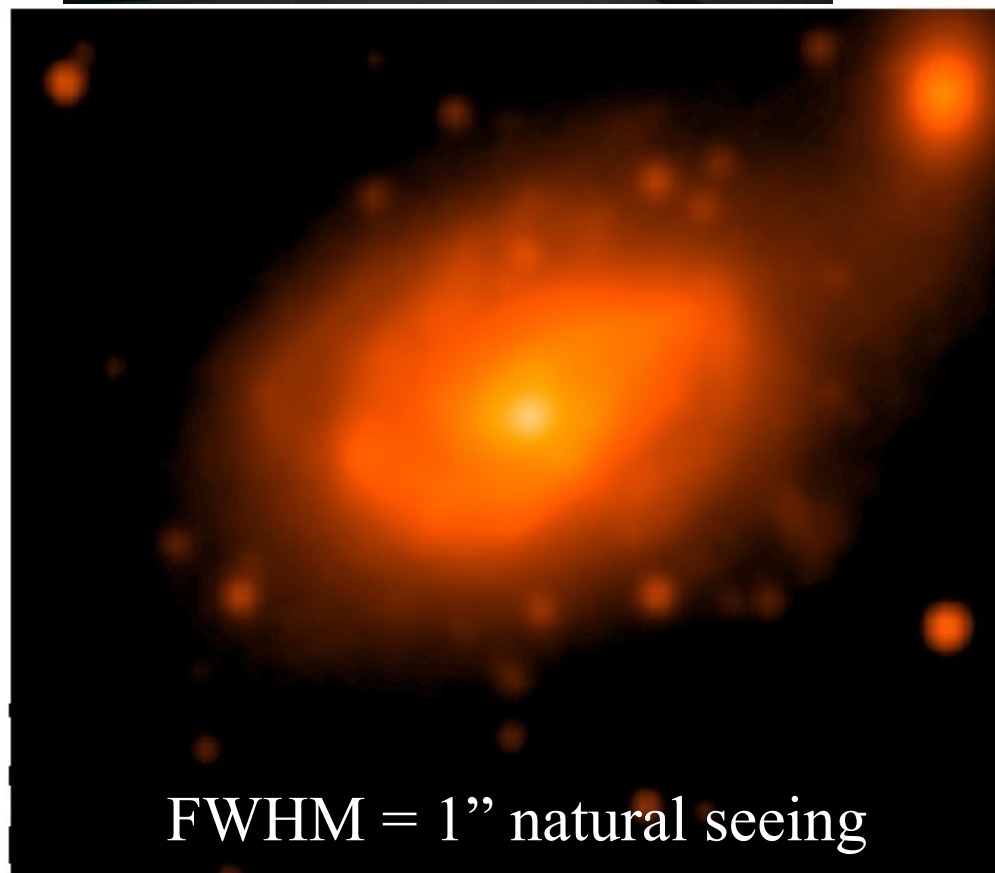
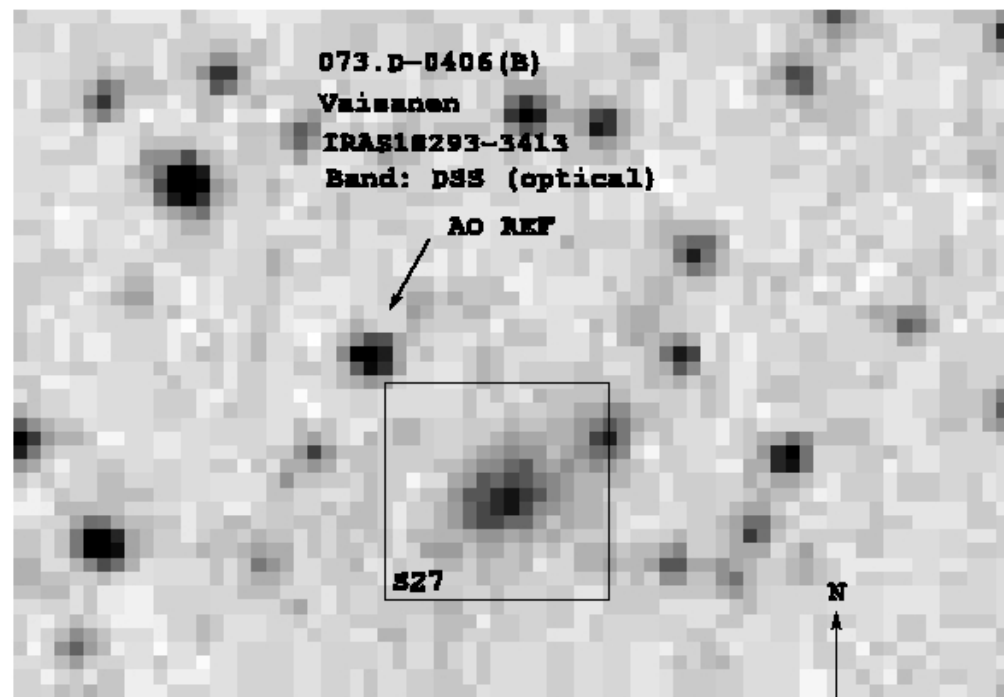
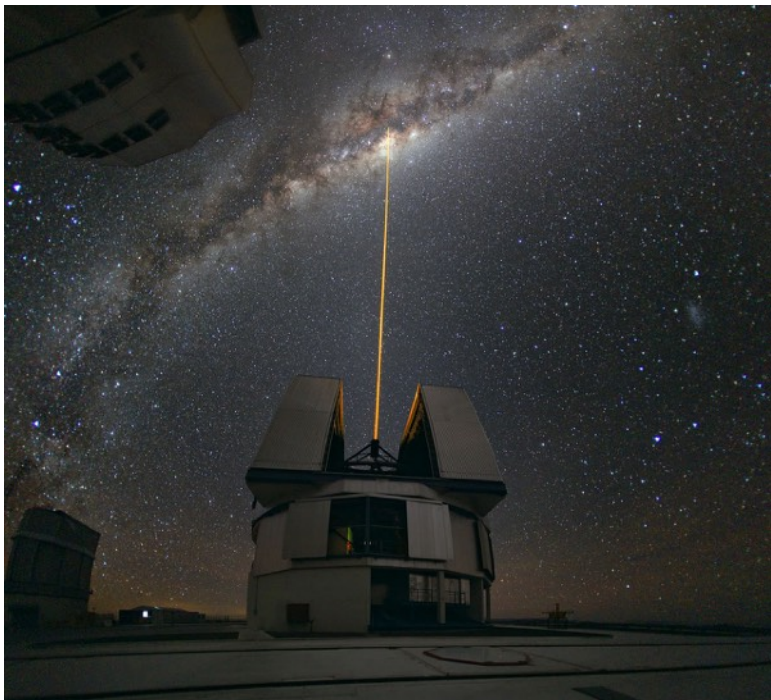


Shack-Hartmann WFS

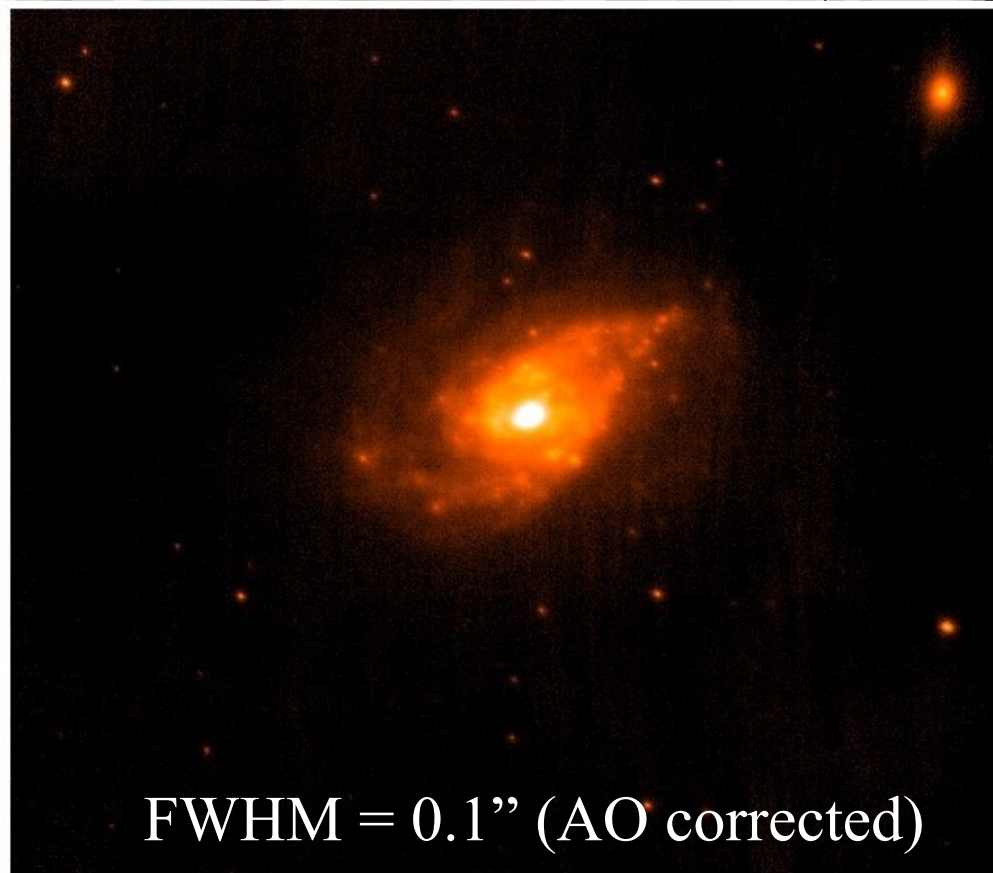


The principles of Adaptive Optics



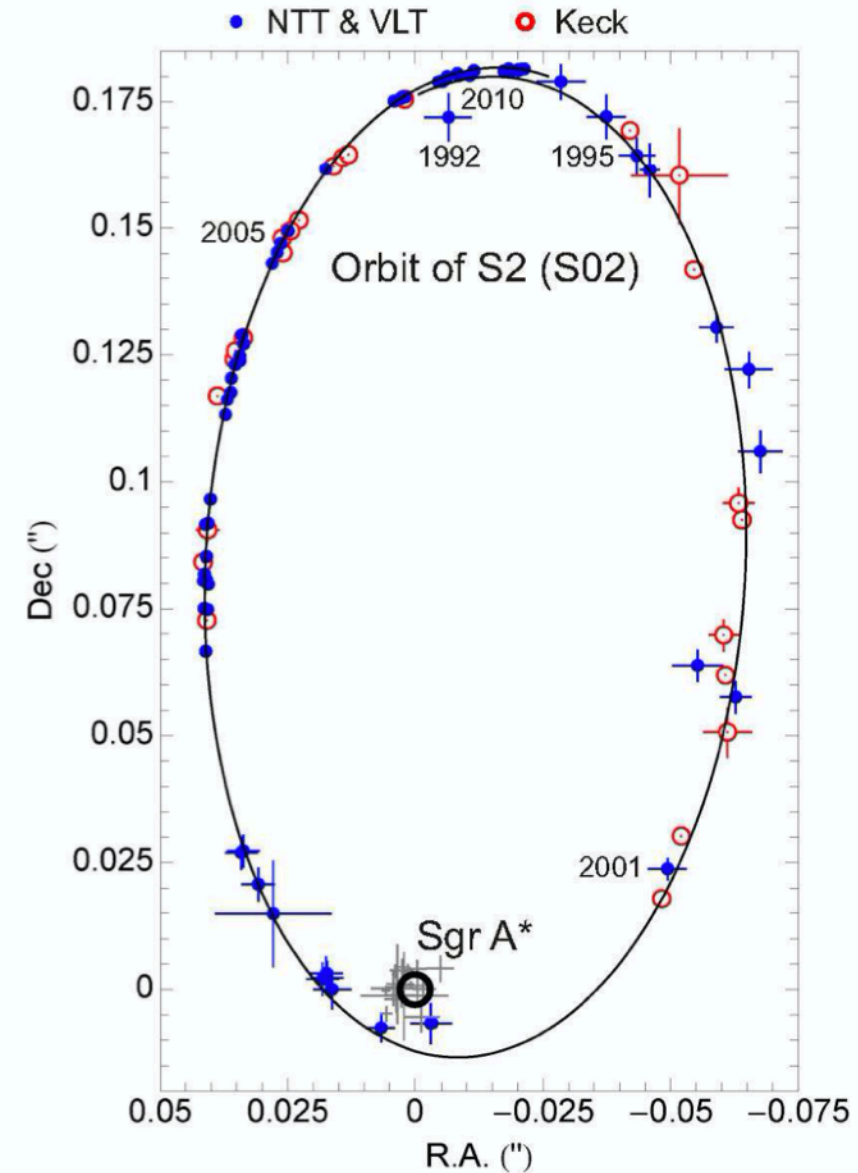
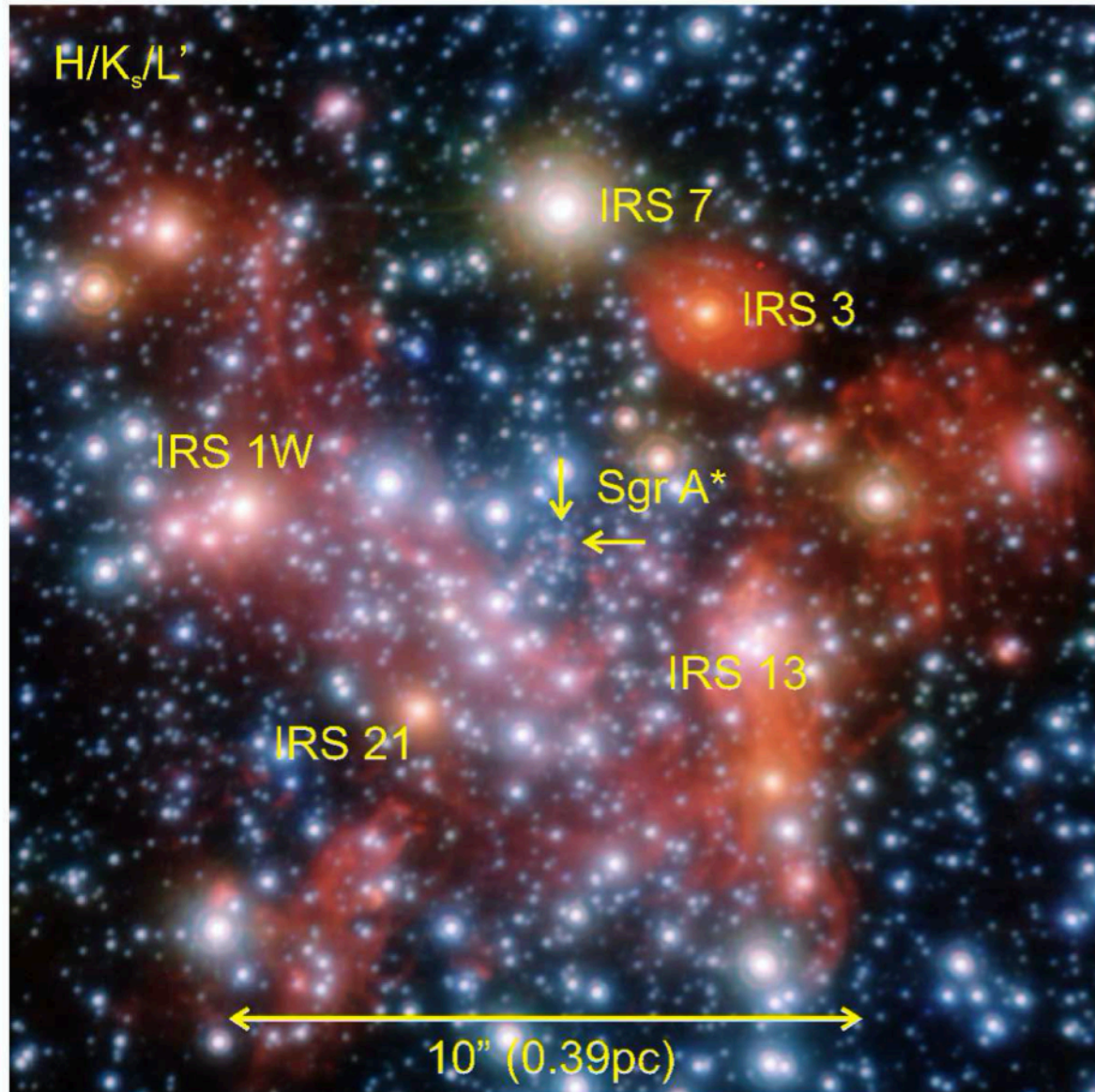


FWHM = 1" natural seeing



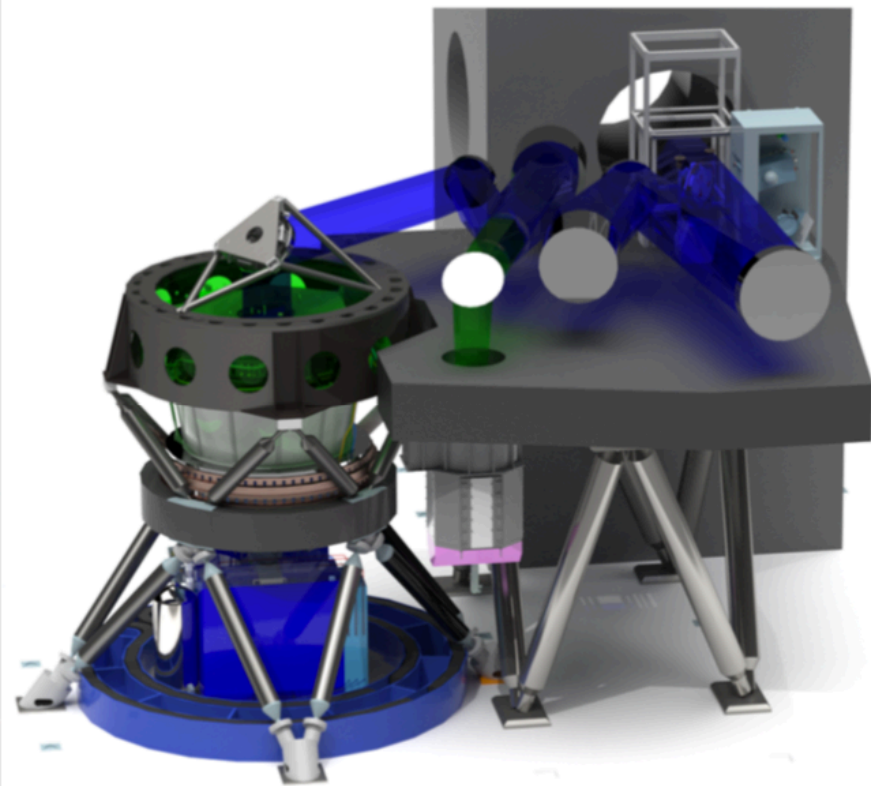
FWHM = 0.1" (AO corrected)

The motion of a star around the central black hole in the Milky Way

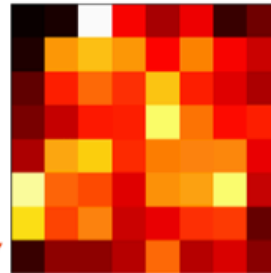


Multi-AO Imaging Camera for Deep Observations (MICADO) will enable ELT to perform diffraction limited: observations $\theta \sim 1.22 \times \lambda / D$

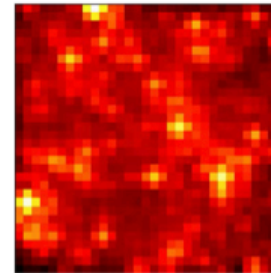
- 4 mas pixel scale providing 50'' x 50'' field of view with fully sampled diffraction limited PSF of the 39-m diameter ELT (FWHM = 12 mas at 2 μm)



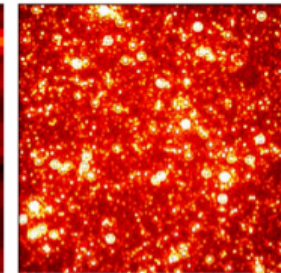
HST / WFC3



JWST / NIRCcam



ELT / MICADO



$\mu=19.6$
(10^6 stars/arcsec²)

